



**HAL**  
open science

## Activated microglia impairs neuroglial interaction by opening Cx43 hemichannels in hippocampal astrocytes

Verónica Abudara, Lisa Roux, Glenn Dallérac, Isabelle Matias, Jérôme Dulong, Jean Pierre Mothet, Nathalie Rouach, Christian Giaume

### ► To cite this version:

Verónica Abudara, Lisa Roux, Glenn Dallérac, Isabelle Matias, Jérôme Dulong, et al.. Activated microglia impairs neuroglial interaction by opening Cx43 hemichannels in hippocampal astrocytes. *Glia*, 2015, 63 (5), pp.795-811. 10.1002/glia.22785 . hal-02626877

**HAL Id: hal-02626877**

**<https://hal.science/hal-02626877>**

Submitted on 8 Jul 2022

**HAL** is a multi-disciplinary open access archive for the deposit and dissemination of scientific research documents, whether they are published or not. The documents may come from teaching and research institutions in France or abroad, or from public or private research centers.

L'archive ouverte pluridisciplinaire **HAL**, est destinée au dépôt et à la diffusion de documents scientifiques de niveau recherche, publiés ou non, émanant des établissements d'enseignement et de recherche français ou étrangers, des laboratoires publics ou privés.



Distributed under a Creative Commons Attribution - NonCommercial 4.0 International License

# Activated Microglia Impairs Neuroglial Interaction by Opening Cx43 Hemichannels in Hippocampal Astrocytes

Verónica Abudara,<sup>1,2,3,4</sup> Lisa Roux,<sup>1,2,3</sup> Glenn Dallérac,<sup>1,2,3</sup> Isabelle Matias,<sup>5,6</sup>  
Jérôme Dulong,<sup>5,6</sup> Jean Pierre Mothet,<sup>5,6,7</sup> Nathalie Rouach,<sup>1,2,3</sup> and Christian Giaume<sup>1,2,3</sup>

<sup>1</sup>Collège de France, Center for Interdisciplinary Research in Biology (CIRB)/Centre National de la Recherche Scientifique, Unité Mixte de Recherche 7241/Institut National de la Santé et de la Recherche Médicale U1050, Paris Cedex, France

<sup>2</sup>University Pierre et Marie Curie, ED, Paris, France

<sup>3</sup>MEMOLIFE Laboratory of Excellence and Paris Science Lettre Research University, Paris, France

<sup>4</sup>Departamento de Fisiología, Facultad de Medicina, Universidad de la República, Montevideo, Uruguay

<sup>5</sup>INSERM U862, Neurocentre Magendie, 33077 Bordeaux, France

<sup>6</sup>Université de Bordeaux, Bordeaux, France

<sup>7</sup>Aix-Marseille Université, CNRS, CRN2M UMR 7286, Marseille, France

Lisa Roux and Glenn Dallérac contributed equally to the work.

Glia plays an active role in neuronal functions and dysfunctions, some of which depend on the expression of astrocyte connexins, the gap junction channel and hemichannel proteins. Under neuroinflammation triggered by the endotoxin lipopolysaccharide (LPS), microglia is primarily stimulated and releases proinflammatory agents affecting astrocytes and neurons. Here, we investigate the effects of such microglial activation on astrocyte connexin-based channel functions and their consequences on synaptic activity in an *ex vivo* model. We found that LPS induces astroglial hemichannel opening in acute hippocampal slices while no change is observed in gap junctional communication. Based on pharmacological and genetic approaches we found that the LPS-induced hemichannel opening is mainly due to Cx43 hemichannel activity. This process primarily requires a microglial stimulation resulting in the release of at least two proinflammatory cytokines, IL-1 $\beta$  and TNF- $\alpha$ . Consequences of the hemichannel-mediated increase in membrane permeability are a calcium rise in astrocytes and an enhanced glutamate release associated to a reduction in excitatory synaptic activity of pyramidal neurons in response to Schaffer's collateral stimulation. As a whole our findings point out astroglial hemichannels as key determinants of the impairment of synaptic transmission during neuroinflammation.

**Key words:** astroglia, gap junctions, neuroinflammation

## Introduction

Neuroinflammation is a widespread response of the brain facing a pathological situation. This process is associated with reactive gliosis characterized by phenotypic changes of glial cells including microglial activation (Hanisch and Kettenmann, 2007) and astrocyte reactivity (Sofroniew, 2005). In health and disease situations, glial cells are active partners of neurons with whom they establish tight interactions, interfering with their activity and survival (Bessis et al., 2007; Parrupura et al., 2012; Rossi and Volterra, 2009). Interestingly, as astrocytes are targets of microglial products and form interacting domains with neurons, notably at the so-called “tripartite

synapse” (Araque et al., 1999), they play a key role in pathological context.

A typical feature of astrocytes is their high level of connexin (Cx) expression (Giaume et al., 2010) that directly impacts synaptic activity (Pannasch et al., 2011) and neuronal survival (Froger et al., 2010), and those channel functions are regulated according to the reactive status of microglia (Retamal et al., 2007). The two Cxs mainly expressed in astrocytes, Cx43 and Cx30, form hexamers that once at the membrane provide the molecular basis for two channel functions: gap junction channels (GJCs) allowing direct cytoplasm-to-cytoplasm communication, and hemichannels (HCs) that

support the release as well as the uptake of ions and small molecules (Bennett et al., 2003; Ransom and Giaume, 2013). Recently, using culture and brain slice models, we reported that acute treatment with the amyloid  $\beta$  peptide activates primarily microglial cells and leads to neuronal death through a mechanism involving astroglial Cx43 HCs (Orellana et al., 2011). Moreover, neuroinflammation triggered by *Staphylococcus aureus* infection leads to region-dependent alterations in astrocyte GJC and HC activities (Karpuk et al., 2011). In these two studies the contribution of another membrane protein family, the pannexins (Panxs), was also shown to be involved in glial HC function. However, so far nothing is known about the impact of astroglial HC activation on synaptic activity in the context of neuroinflammation.

In co-cultures, selective activation of microglia by a low concentration of LPS induces an opposite regulation of the two Cx channel functions in astrocytes: HC activity is increased while GJC communication is reduced (Retamal et al., 2007). Here, we aimed to determine whether such mechanisms occur in a more integrated model represented by acute hippocampal slices, and to identify their impact on synaptic activity. We found that LPS treatment induces HC activity mainly due to Cx43 HC opening as revealed by the ethidium bromide (Etd) uptake technique (see Giaume et al., 2012). This effect requires microglial activation and the release of at least two identified proinflammatory cytokines. The opening of astrocyte Cx43 HCs results in increased levels of intracellular calcium ( $[Ca^{2+}]_i$ ) and extracellular glutamate concentrations associated to a decrease in excitatory synaptic transmission in the CA1 area of the hippocampus. As microglial activation and alteration of neurotransmission are two early symptoms of many brain pathologies (Giaume et al., 2007; Verkhratsky et al., 2012), these observations provide a basis to further understand the contribution of glia to neuronal dysfunction in neuroinflammation and brain diseases. Accordingly, this work could open the way for alternative therapeutic strategies targeting astroglial Cx hemichannels to prevent, or at least attenuate, neuronal damage associated to brain inflammation.

## Methods

### Animals

Slices and cultures were obtained from wild-type C57BL/6 and transgenic mice (P17–P40) including GFAP-eGFP mice, Cx30(–/–) knockout mice, Cx43(fl/fl):GFAP-cre mice, a conditional knockout for astrocyte Cx43, and the double knockout for astrocyte Cx43 and Cx30, Cx30(–/–)Cx43(fl/fl):GFAP-cre mice. All experiments were performed at the age when both Cxs are expressed in control condition (Kunzelmann et al., 1999).

All experiments were performed according to the European Community Council Directives of January 1, 2013 (2010/63/EU)

and all efforts were made to minimize the number of animals used and their suffering.

### Hippocampal Slices

Wild-type C57BL/6 and transgenic mice (20- to 28-day old) were decapitated and the brain was rapidly removed. Hippocampi were dissected and placed in ice-cold artificial cerebrospinal fluid (ACSF) equilibrated with 95% O<sub>2</sub> and 5% CO<sub>2</sub>. Transverse hippocampal slices (300–400  $\mu$ m thick) were cut with a vibroslicer (Leica VT 1000S, Wetzlar, Germany) and transferred to a storage chamber where they rested on a nylon mesh, submerged in oxygenated ACSF at room temperature (RT) for a stabilization period of 45 min. The ACSF solution contained in mM: NaCl 134; KCl 2.8; NaHCO<sub>3</sub> 29; NaH<sub>2</sub>PO<sub>4</sub> 1.1; glucose 12; MgSO<sub>4</sub> 1.5; CaCl<sub>2</sub> 2.5. In order to assess cellular viability and membrane integrity in control and LPS treated conditions, slices were incubated in ACSF containing Ethidium homodimer (Etd-1, 857 Da. Life Technologies (Molecular Probes) 200 nM for 15 min at RT. Then, slices were rinsed, incubated in fixing solution for 2 h (4% paraformaldehyde in 0.12 M buffer phosphate) and mounted in Fluoromount-G mounting medium until photomicrographs were taken. Labeled cells were visualized with a confocal laser-scanning microscope (Leica TBCS SP2). The fluorescent cell-impermeant viability indicator Etd-1 emits strong red fluorescence (excitation/emission maxima  $\sim$ 528/617 nm) only when bound to DNA. This indicator stains all of the dead or dying cells experiencing disrupted membranes and not only those undergoing programmed cell death. Using this indicator we could not detect highly fluorescent dead cells in slices when using the Etd-1 viability test at depths distant from the surface ( $>10$   $\mu$ m) either in control or LPS-treated slices.

### Dye Uptake Experiments

In slices derived from GFAP-eGFP mice, astrocytes were identified by GFP fluorescence (Nolte et al., 2001). Alternatively, astrocytes were also identified by GFAP immunoreactivity (see below). Living slices were incubated with the HC permeable fluorescent tracer ethidium bromide (Etd, 314 Da) for 10 min at RT and at 4  $\mu$ M final concentration. Slices were treated for 3 h either with lipopolysaccharide (LPS, 1–100 ng/mL), or with or without a mixture of proinflammatory cytokines (Mix) of interleukin-1 $\beta$  (IL-1 $\beta$ ) and tumor necrosis factor- $\alpha$  (TNF- $\alpha$ ; 20 ng/mL each); otherwise proinflammatory cytokines were applied separately when indicated. To determine the sensitivity of Etd uptake to Panx1 HCs or Cx HCs blockers, slices were incubated before and during dye application with the Cx HC blocker La<sup>3+</sup> (400  $\mu$ M), the Cx HC/Px HC blocker carbenoxolone (CBX, 100–200  $\mu$ M), the selective antagonist of P2X<sub>7</sub> receptors Brilliant Blue G (BBG, 1  $\mu$ M) or with mimetic blocking peptides against Cx43 or Panx1, Gap26 (0.16 mM), and <sup>10</sup>Panx1 (0.4 mM). In blocking experiments, 15 min before and during LPS, slices were treated with an inhibitor of microglial activation, minocycline (10–100 nM) or with the soluble TNF- $\alpha$  receptor (sTNF- $\alpha$ R1) and IL-1 $\beta$  receptor (IL-1ra) antagonists (200 ng/mL each). Following the 10 min incubation with Etd, slices were rinsed 15 min in ACSF to stop the uptake and reduce background labeling before submerging them for 2 h in fixing solution (4% paraformaldehyde in 0.12 M

buffer phosphate). Fixed slices were then rinsed in PBS and mounted in Fluoromount-G mounting medium until photomicrographs were taken. Labeled cells were visualized with a 40 $\times$  objective in a microscope equipped with epifluorescence illumination and appropriate filters for Etd (excitation wavelength, 528 nm; emission wavelength, 598 nm) and GFAP-eGFP (excitation wavelength, 488 nm; emission wavelength, 507 nm). Alternatively, immunolabeled astrocytes were examined at 63 $\times$  and 20 $\times$  with a confocal laser-scanning microscope (Leica TBCS SP2). Stacks of consecutive confocal images taken at 1  $\mu$ m intervals were acquired sequentially with two lasers (argon 488 nm for GFAP-eGFP and 561 nm for Etd). Fluorescence was quantified in arbitrary units (AU) with image processing software Adobe Photoshop (Adobe Systems Software Ireland Ltd.). Dye uptake intensity was evaluated as the difference ( $F - F_0$ ) between the fluorescence ( $F$ ) from astrocytes (20–30 cells per slice) and the background fluorescence ( $F_0$ ) measured in the same field where no labeled cells were detected. At least three fields were selected in every slice for background evaluation.

### Dye Coupling Experiments in Slices

Acute hippocampal slices were prepared as previously described from 3 week-old wild-type C57BL/6 and transgenic Cx30(-/-) mice (Orellana et al., 2011). For dye coupling experiments, slices were transferred in a recording chamber mounted on the fixed stage of an up-right microscope (Axioskop FS, Zeiss, Oberkochen, Germany) equipped with Nomarski optics and an infrared CCD video camera (Pixelfly QE, The Cook Corporation, Romulus, MI) while continuously perfused with oxygenated ACSF at a rate of 2 mL/min at RT. Cells within the CA1 *stratum radiatum* of the hippocampus were identified as astrocytes based on morphological criteria and electrophysiological properties. They were recorded in whole-cell configuration using 10 to 15 M $\Omega$  glass electrodes filled with (in mM): 105 K-gluconate, 30 KCl, 10 HEPES, 10 Phospho-creatine Tris, 4 ATP-Mg, 0.3 GTP-Tris, 0.3 EGTA (pH 7.3; 280 mOsm). Patch-clamp recordings (10 kHz sampling and 2 kHz filtering) were performed with Pclamp9 software (Molecular Devices, Foster City, CA), membrane voltages and currents were amplified by a MultiClamp 700B amplifier and sampled by a Digidata 1322A Interface. Input resistance ( $R_{in}$ ) was measured in voltage-clamp mode by applying hyperpolarizing voltage pulses (10 mV, 150 ms) from a holding potential of -80 mV. To evaluate the level of coupling, sulforhodamine B (559 Da; 1 mg/mL; Invitrogen, Eugene, OR) was added in the intracellular solution and loaded in the recorded cells during 15 min in current-clamp mode. Intercellular diffusion of sulforhodamine B was captured thereafter with the CCD camera (Pixelfly QE, The Cook Corporation, Romulus, MI) and the number of sulforhodamine B positive cells (i.e. cells coupled to the recorded astrocyte) was determined using Image J software as previously described (Roux et al., 2011).

### Electrophysiology

Slices (400  $\mu$ m thick) were treated during 3 h with LPS (50 ng/mL); in some experiments mimetic blocking peptides, Gap26 (0.16 mM) and <sup>10</sup>Panx1 (0.4 mM) were applied 15 min before and during LPS exposure. For synaptic recordings, a cut was made

between the CA3 and CA1 region to prevent bursting, and slices were bathed in a modified ACSF containing 100  $\mu$ M picrotoxin to block GABA<sub>A</sub> receptor-mediated inhibitory postsynaptic currents. Field excitatory postsynaptic potentials (fEPSPs) were recorded in CA1 area with glass pipettes (2–5 M $\Omega$ ) filled with ACSF, and evoked by stimulating Schaffer collaterals in *stratum radiatum* (0.1 Hz) with a monopolar stimulating electrode. Recordings were acquired with Axopatch-1D amplifier (Axon Instruments, Molecular Devices, Sunnyvale, CA), filtered at 2 kHz, digitized at 10 kHz, and analyzed online using Clampfit software (Molecular Devices).

### Immunofluorescence

For identification of astrocytes and activated microglia, slices were incubated for 2 h in fixing solution (4% paraformaldehyde in 0.12 M buffer phosphate). They were then rinsed twice for 15 min with PBS and incubated for 1 h in agitation at RT in a blocking solution containing 0.25% Triton X-100 and 2 g/L gelatin in PBS (PBS/Gel/Triton). Slices were then incubated overnight at 4°C with primary antibodies mouse GFAP (Sigma clone GA-5, 1/500) or rabbit GFAP (Sigma, 1:500) and monoclonal rat anti-CD11b (M1/70; BD Biosciences, 1/200). Subsequently, slices were rinsed twice for 30 min in PBS/Gel/Triton and incubated in dark in the secondary antibody (Alexa 488 anti-rabbit or anti-mouse, 1:2,000 for GFAP and anti-rat rhodamine conjugated, 1/250 for CD11b) for 1.5 h diluted in the same medium. Following several washes in PBS, slices were mounted in mounting medium (Fluoromount-G) and examined with a confocal laser-scanning microscope (Leica TBCS SP2). Stacks of consecutive confocal images taken at 300 nm intervals were acquired sequentially with two lasers (argon 488 nm for GFAP and 561 nm for CD11b) Z projections were reconstructed using the LAS AF Software.

### Intracellular Calcium Measurements

Acute brain slices derived from wild-type C57BL/6 and double knockout Cx30(-/-)Cx43(fl/fl):GFAP-cre mice were incubated for 50 to 60 min in dark at 37°C in ACSF containing 0.02% Pluronic F-127 and the calcium indicator Fluo-4/AM (5  $\mu$ M) which has been demonstrated to load specifically astrocytes (Hirase et al., 2004). Astrocytes were further identified by their ability to uptake the fluorescent tracer sulforhodamine 101 (SR 101; Kafitz et al. 2008; Schnell et al., 2012). Briefly, living slices were incubated in dark for 20 min at 34°C in ACSF solution containing SR 101 at 1  $\mu$ M final concentration. After dye-loading, slices were thoroughly washed by a 20 min incubation in normal ACSF solution (equilibrated with 95% O<sub>2</sub> to 5% CO<sub>2</sub>). As illustrated in Fig. 5A, SR 101 labeling colocalized with Fluo-4/AM labeling in astrocytes. Pyramidal neurons were not labeled by Fluo-4/AM (not shown). Preparations were then subjected to 3 h treatment with either LPS (50 ng/mL), or interleukin-1 $\beta$  (IL-1 $\beta$ ; 20 ng/mL), or tumor necrosis factor- $\alpha$  (TNF- $\alpha$ ; 20 ng/mL) or with a mixture of these proinflammatory cytokines in dark until [Ca<sup>2+</sup>]<sub>i</sub> measurements were made. In blocking experiments, slices were incubated 15 min before and during LPS or cytokines treatment with minocycline (50 nM) or with mimetic peptides Gap26 (0.16 mM) plus <sup>10</sup>Panx1 (0.4 mM) or with the cytokine inhibitors, the soluble TNF- $\alpha$  receptor

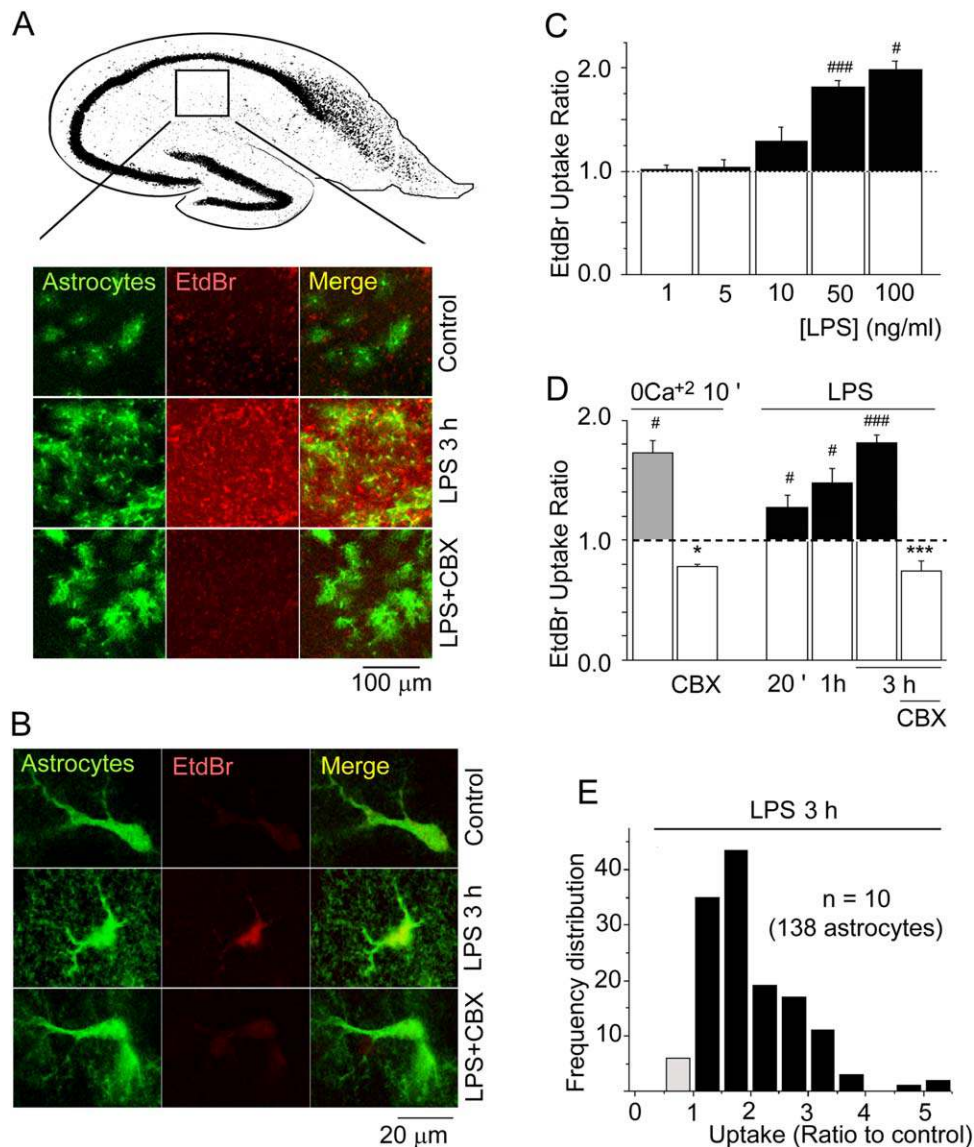


**FIGURE 1: LPS treatment increases ethidium bromide uptake through astrocyte hemichannels in acute hippocampal slices. (A)** Fluorescence representative contrasted images of acute hippocampal slices derived from GFAP-eGFP transgenic mice show GFAP-eGFP (green) astrocytes and Etd uptake (red) under control conditions (control), under exposure to LPS (50 ng/mL) alone (LPS) and in presence of the CxHC and Panx channel blocker carbenoxolone (200  $\mu$ M) applied 15 min before and during dye uptake measurement (LPS + CBX). Images of hippocampal astrocytes were taken from the CA1 interpyramidal zone (CA1 stratum radiatum) as depicted by the square in the upper scheme of a hippocampal slice. **(B)** Higher magnification showing Etd uptake in a single GFAP-eGFP-positive astrocyte in similar conditions that in A. **(C)** Averaged data normalized to control (dashed line) of Etd uptake rate in GFAP-eGFP positive hippocampal astrocytes treated for 3 hours with different doses of LPS (1–100 ng/mL). ###  $P < 0.001$  and #  $P < 0.05$ : significant increases compared with control condition without treatment (two-tailed Wilcoxon signed-rank test). **(D)** Averaged data normalized to control (dashed line) of Etd uptake rate in GFAP-eGFP positive hippocampal astrocytes in the absence of extracellular calcium ( $0Ca^{2+}$ ; 10 min) or treated with LPS alone (50 ng/mL) for different time periods (20 min; 1 h; 3 h) or with LPS (50 ng/mL, 3 h) in presence of CBX applied 15 min before and during Etd uptake measurements (LPS + CBX). #  $P < 0.05$  and ###  $P < 0.001$  indicate significant increases compared with control condition without treatment (two-tailed Wilcoxon signed-rank test). \*  $P < 0.05$ , \*\*\*  $P < 0.001$ , effect of CBX compared with the effect induced by respectively  $0Ca^{2+}$  or 3 h of LPS alone on Etd uptake (two-tailed Mann-Whitney  $U$ -test). Note that Etd uptake is similar in absence of extracellular calcium and after 3 h of LPS treatment ( $P > 0.05$ , two-tailed Mann-Whitney  $U$ -test). **(E)** Relative frequency distribution of the Etd uptake ratio by hippocampal astrocytes under LPS treatment (50 ng/mL, 3 h). Note that in all experiments CBX was applied 15 min before and during Etd uptake measurements. All averaged data are obtained from 3 to 17 independent experiments in C and D, and from 138 astrocytes (10 independent experiments) in E.

(sTNF- $\alpha$ R1) and IL-1 $\beta$  receptor (IL-1ra) antagonists (300 ng/mL each). Then, slices were transferred to the recording chamber of an Olympus BX51WI microscope. Fluo-4 and SR 101 were excited at

respectively 488 nm and 587 nm through a light emitting diode, controlled by the Axon Imaging Workbench software. Fluorescent emission of labeled cells at 515 nm (Fluo-4/AM) and 602 nm

(SR 101) was detected with an EM-CCD camera (Andor, Belfast, UK). Images were acquired every 30 to 60 s through a 20× water immersion objective (NA 0.95, Olympus, Japan) and stored on a PC. Offline analysis of images was processed with AIW imaging software.

### Determination of L-Glutamate Extracellular Levels by CE-LIF

Extracellular levels of L-glutamate were determined from acute hippocampal slices ( $n = 3$  slices/tube/condition) incubated in oxygenated ACSF as recently described (Fossat et al., 2012). After equilibration, samples of extracellular medium were collected at 0, 60 and 180 to min intervals after addition of the compounds and directly frozen in liquid nitrogen and stored at  $-80^{\circ}\text{C}$  until analysis. Intracellular levels of L-glutamate in hippocampal slices were also analyzed. Briefly, pooled slices were first deproteinized by addition of cold trichloroacetic acid to a 5% final concentration. The suspension was centrifuged at  $16,800g$  for 10 min, and the TCA was extracted from the supernatant with water-saturated diethyl ether and stored at  $-80^{\circ}\text{C}$  until analysis. Analyses of the samples were performed with a commercial laser-induced fluorescence capillary electrophoresis (CE-LIF; CE: Beckman Coulter, P/ACE MDQ; LIF: Picometrics, LIF-UV-02, 410 nm 20 mW) as following. The samples were processed for micellar CE-LIF and were fluorescently derivatized at RT for 60 min with naphthalene-2,3-dicarboxaldehyde (NDA) before being analyzed by CE using a hydroxypropyl- $\beta$ -cyclodextrin (HP- $\beta$ -CD) based chiral separation buffer. All electropherograms data were collected and analyzed using Karat 32 software v8.0 (Beckman Coulter, Fullerton, CA). Further analysis was made using GraphPad Prism 4.03 software.

The extracellular and intracellular amounts of L-glutamate were normalized to the protein content determined from pooled hippocampal slices by the Lowry method using the BCA protein Pierce (ThermoScientific, CA) assay with bovine serum albumin (BSA) as standards. The quantity of L-glutamate in the samples was determined from a standardized curve while peak identification was made by spiking the fraction with the amino acid. For accurate comparison between conditions extracellular levels of L-glutamate (referred here as  $[\text{glu}]_{\text{ext}}$ ) was normalized to total L-glutamate (intracellular + extracellular; referred here as  $[\text{glut}]_{\text{tot}}$ ) allowing us to assess the released fraction of L glutamate (see legend of Fig. 7).

### Statistical Analysis

Values are presented as mean values  $\pm$  SEM;  $n$  expresses the number of independent experiments. Detailed statistical results were included in the figure legends. Except for the determination of L-glutamate levels and unless otherwise stated, in all experiments where the effects of different treatments were assessed on normalized data, non-parametric ANOVA Kruskal-Wallis tests were performed. Tests with significant  $P$  value ( $<0.05$ ) were followed by a Dunn's multiple comparison *post hoc* test using the GraphPad Prism version 5.00 (San Diego, CA). Unless otherwise stated, significance as compared with control condition based on the raw data (before normalization) was assessed by two-tailed Wilcoxon signed-ranked tests. The level of significance was set at  $P < 0.05$ . Graphics were prepared using

Microcal Origin 6.0 (Northampton, MA) and Adobe Illustrator 10 (San Jose, CA). For extracellular determination of L-glutamate, statistical analysis and curves fittings were performed using GraphPad Prism 4.03. Data were fitted using a polynomial second order non-linear regression and statistical significance between conditions was determined at  $P < 0.05$  using an ANOVA followed by Newman-Keuls Multiple Comparison Test or using Student's  $t$ -test.

## Results

### LPS Activates Hemichannels in Astrocytes from Acute Hippocampal Slices

Hemichannel activity was studied by ethidium bromide (Etd) uptake in fluorescent astrocytes located in the CA1 region of acute hippocampal slices (*stratum radiatum*) from GFAP-eGFP mice (Fig. 1A). After 3 h exposure to LPS (50 ng/mL), Etd uptake in GFAP-eGFP positive cells was on average about twice stronger (181% of control,  $n = 17$ ) than the uptake measured in control conditions (Fig. 1A–E). Under these conditions, the majority of eGFP-positive astrocytes exhibited an enhanced Etd uptake (Fig. 1E). Importantly, the uptake in eGFP-positive astrocytes was dependent on the concentration (Fig. 1C) and the duration (Fig. 1D) of LPS treatment. Indeed, LPS concentration was found to be effective in increasing Etd uptake in the range of 50 to 100 ng/mL, and required at least 3 h treatment for a concentration of 50 ng/mL (Fig. 1C,D). This effect was suppressed by carbenoxolone (CBX, 200  $\mu\text{M}$ ), a gap junction channel (GJC), and hemichannel (HC) inhibitor, applied 15 min before and during LPS treatment, demonstrating that Etd uptake occurred through HCs (Fig. 1A,B,D). Lower concentrations of carbenoxolone (100 and 150  $\mu\text{M}$ ) were also found to be effective in blocking LPS-induced uptake of Etd (data not shown). Note that when exposed to CBX, the Etd uptake level was under the control level line indicating that in basal condition HCs are already active in hippocampal astrocytes as recently reported (Chever et al., 2014). Finally, as a positive control for HC opening, short-term exposure (10 min) of slices to a calcium free solution (0  $\text{Ca}^{2+}$  and 5 mM EGTA) was used (Ye et al., 2003). In this condition, the increase in Etd uptake was similar to the one monitored after 3 h LPS (50 ng/mL) treatment, and was also suppressed by CBX pretreatment (Fig. 1D). Altogether these observations indicate that LPS-induced inflammatory treatment activates HCs in astrocytes from acute hippocampal slices.

An inhibition of dye coupling has been reported in cortical astrocytes cultured with LPS-activated microglia (Même et al., 2006; Retamal et al., 2007). Accordingly, a potential change in GJC-mediated coupling of LPS-treated hippocampal slices was investigated by performing dye coupling experiments. To assess the level of gap junctional communication, whole-cell recordings from astrocytes identified by their typical electrophysiological properties (i.e. a “passive” current/voltage

relationship, a low input resistance and a highly negative resting membrane potential of about  $-80$  mV) were performed with patch-clamp pipettes containing sulforhodamine B, a GJC permeable dye. In control conditions, after 15 min dialysis,  $19 \pm 1$  neighboring cells ( $n = 11$ ) were stained by sulforhodamine B (Fig. 2A). Interestingly, the extent of this dye coupling was unchanged ( $18 \pm 3$ ,  $n = 6$ ) with LPS treatment (50 ng/mL, 3 h), unlike results obtained in primary cell cultures (Même et al., 2006; Retamal et al., 2007). Astrocytes in primary culture or in co-culture with microglia express only Cx43, while *in vivo*, they also express Cx30 after postnatal day 12–15 in rodents (Kunzelmann et al., 1999; Koulakoff et al., 2008; Nagy and Rash, 2000). Accordingly, the absence of LPS effect on dye coupling could be due to the presence of Cx30 compensating for the potential inhibition of Cx43 GJC-mediated dye coupling. To investigate this possibility, dye coupling assays were also performed in hippocampal slices from Cx30 knock-out mice (Teubner et al., 2003). As already reported (Gosejacob et al., 2011; Rouach et al., 2008), in these animals dye coupling was significantly reduced by 33 % ( $n = 6$ ) compared with control conditions, due to the lack of Cx30 GJCs (Fig. 2B). However, no difference in the intercellular diffusion of the dye was detected between control ( $13 \pm 2$ ,  $n = 5$ ) and LPS treated slices ( $16 \pm 2$ ,  $n = 6$ ) from Cx30 $-/-$  mice (Fig. 2A,B). This indicates that, in contrast to HCs, neither Cx43 nor Cx30 astroglial GJCs are affected by LPS treatment in hippocampal slices. Interestingly, membrane potential recorded from wild-type control and LPS-treated wild-type astrocytes were  $-86.3 \pm 0.4$  mV ( $n = 11$ ) and  $-85.2 \pm 1.1$  mV ( $n = 5$ ), respectively, and  $-84.4 \pm 1.3$  mV ( $n = 5$ ) and  $-83.9 \pm 0.8$  mV ( $n = 6$ ) for control Cx30KO and LPS-treated Cx30KO astrocytes, respectively. This indicated that LPS treatment activating HCs in astrocytes do not affect the resting membrane potential of hippocampal astrocytes.

### **Cytokines Released by Activated Microglia Induces Hemichannel Opening in Astrocytes**

As illustrated in Fig. 3A, LPS (3 h, 50 ng/mL) induced an activation of microglial cells, as indicated by an increase in the number of CD11b-positive cells. The endotoxin treatment also enhanced GFAP immunoreactivity, as indicated by the higher number of GFAP-positive cells from the GFAP-eGFP mouse and the brighter immunostaining of astrocyte processes (Figs. 1A and 4A). Interestingly, minocycline (50 nM), an inhibitor of microglial activation (Fig. 3A; Pascual et al., 2012; Yrjänheikki et al., 1998), applied 15 min before and during treatment with LPS, abolished astroglial LPS-induced Etd uptake in a dose-dependent manner (Fig. 3B). This observation indicates that under LPS treatment, the activation of microglia is a prerequisite for the activation of

HCs in astrocytes. Moreover, under blocking conditions of minocycline (i.e., doses of minocycline that inhibit Etd uptake in astrocytes), no increase in GFAP immunoreactivity was detected compared with control conditions.

Activation of microglia results in the production of proinflammatory cytokines (Minami et al., 2006; Mizuno et al., 1994), including IL-1 $\beta$  (Giulian et al., 1986) and TNF- $\alpha$  (Sawada et al., 1989; Wood, 1994). We previously reported that, in co-cultures of astrocytes and microglial cells, LPS-induced HC activation in astrocytes was partly due to the release of these two proinflammatory cytokines from activated microglia (Retamal et al., 2007). Accordingly, we investigated whether 3 h exposure of hippocampal slices to IL-1 $\beta$  and TNF- $\alpha$  (20 ng/mL each) mimicked the LPS-induced HC activation in astrocytes. When applied separately, TNF- $\alpha$  and IL-1 $\beta$  provoked significant uptake of Etd (144% and 166%,  $n = 6$ , respectively) but the extent of each cytokine induced-uptake was lower compared with LPS treatment (212%,  $n = 19$ ; TNF- $\alpha$  *vs.* LPS,  $P < 0.0001$  and IL-1 $\beta$  *vs.* LPS,  $P < 0.03$ ; *U*-test). Nevertheless, similarly to LPS-induced Etd uptake, 3 h application of a mixture (MIX) of both cytokines enhanced astrocyte uptake to twice the control levels (210%,  $n = 7$ ). Indeed, the effect induced by simultaneous administration of IL-1 $\beta$  and TNF- $\alpha$  was additive and totally prevented by CBX pre-treatment (Fig. 3B). Moreover, in the presence of specific blockers of each cytokine pathways, i.e. the receptor antagonist IL-1ra and the soluble receptor sTNF- $\alpha$ R1 (300 ng/mL each), LPS no longer increased Etd uptake in eGFP-GFAP-positive hippocampal astrocytes (Fig. 3B). These observations indicate that the release of IL-1 $\beta$  and TNF- $\alpha$  from microglia is required to induce HC activation in astrocytes in the presence of LPS.

### **LPS-Induced Ethidium Bromide Uptake in Astrocytes is Mainly Mediated by Connexin43 Hemichannels**

In LPS-treated hippocampal slices, Etd uptake in astrocytes is completely blocked by CBX (Fig. 1D), indicating that both Cx HCs and/or Panx (already defined) channels could mediate Etd transmembrane transfer (Orellana et al., 2009; Scemes et al., 2009). To discriminate the involvement of these two types of membrane channels, their respective contribution was first tested by their sensitivity to different inhibitors (see Giaume and Theis, 2010; Giaume et al., 2013). As illustrated in Fig. 4, the increase in Etd uptake evoked by LPS treatment (207% of the control,  $n = 20$ ) was strongly inhibited by 400  $\mu$ M La $^{3+}$  (to 130% of the control,  $n = 10$ ), that blocks Cx HCs but does not affect Panx channels (Bruzzone et al., 2005; Pelegrin and Surprenant, 2006; Schalper et al., 2010). This inhibition was similar to the effect induced by CBX that blocks Cx GJCs and HCs as well as Panx channels (to 80%

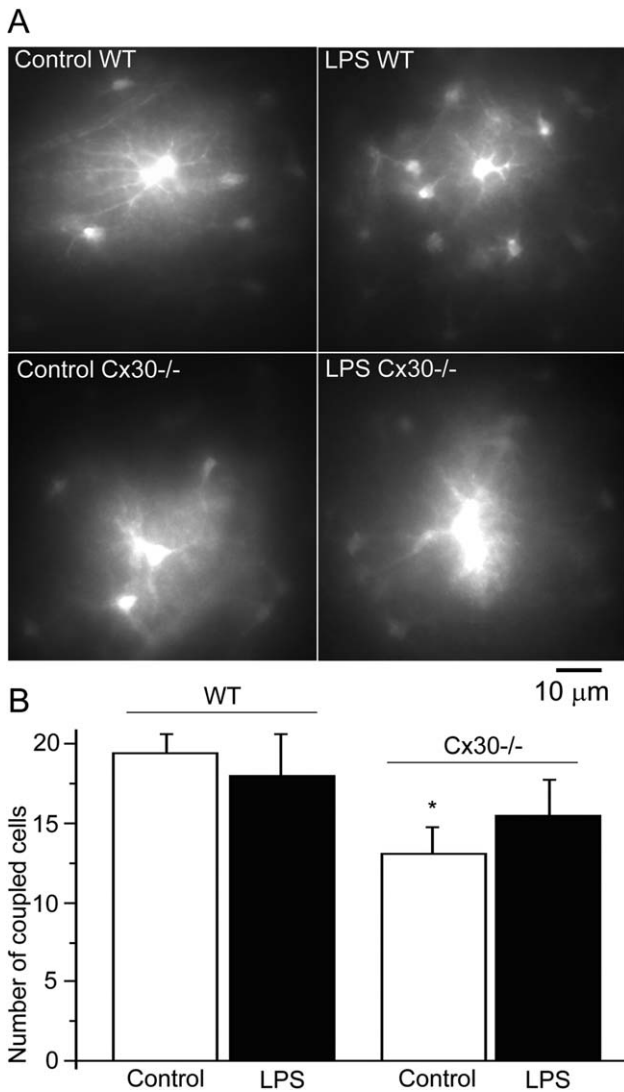


**FIGURE 2:** LPS treatment does not affect gap junctional communication between hippocampal astrocytes in acute slices. **(A)** Fluorescence representative images of dye (sulforhodamine B) coupled astrocytes in acute hippocampal slices derived from non-transgenic C57BL/6 (WT) and Cx30-deficient (Cx30<sup>-/-</sup>) mice under control conditions (control) or treated with LPS (LPS, 50 ng/mL, 3 h). **(B)** Averaged number of coupled cells under same conditions that in **(A)**. The number of coupled cells is significantly reduced in Cx30<sup>-/-</sup> hippocampal slices compared with WT (\* $P < 0.05$ , two-tailed Mann-Whitney  $U$ -test). However, LPS treatment does not impact on the number of coupled cells neither in WT nor in Cx30<sup>-/-</sup> hippocampal slices ( $P > 0.05$ , two-tailed Mann-Whitney  $U$ -test). Data are obtained from 5 to 11 independent experiments.

of the control  $n = 7$ , Fig. 1D). Since the effects of  $\text{La}^{3+}$  and CBX did not statistically differ significantly, Cx HCs must primarily be involved in the Etd uptake triggered by LPS treatment. A potential involvement of Panx1 HCs was, however, further investigated. Since it has been proposed that activation of the purinergic receptors  $\text{P2X}_7\text{R}$  in macrophages induces dye uptake through Panx1-formed channels (Pelegri

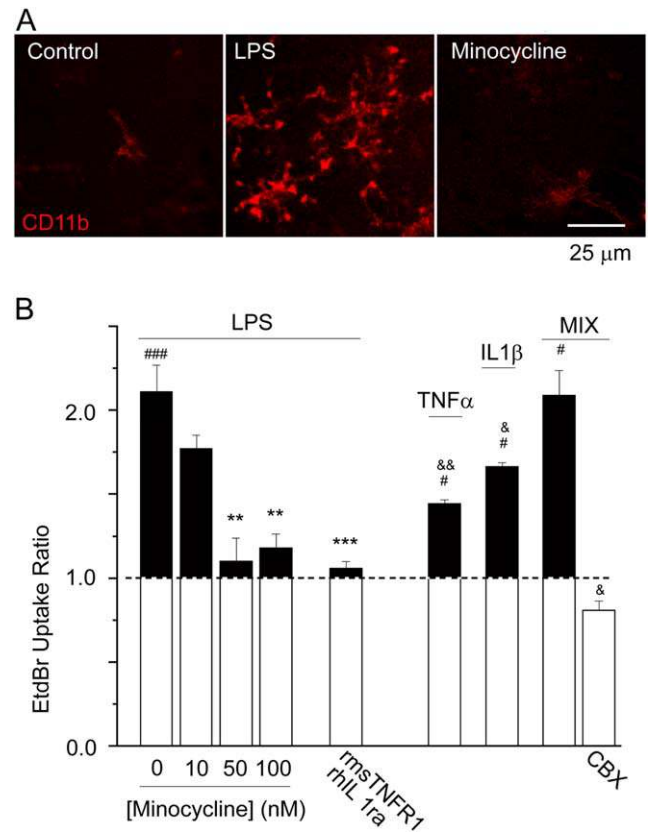


**FIGURE 3:** Release of proinflammatory cytokines TNF- $\alpha$  and IL-1 $\beta$  from activated microglia is required for the LPS-induced Etd uptake in hippocampal astrocytes. **(A)** Immunofluorescence images depicting CD-11B immunolabeling of microglia in hippocampal acute slices under control conditions (Control), after treatment with LPS (50 ng/mL, 3 h) alone (LPS) or in presence of minocycline (50 nM), an inhibitor of microglial activation. Note that fluorescence of CD11B<sup>+</sup> cells is greatly increased under LPS treatment. **(B)** Left, averaged data normalized to control (full line) of Etd uptake rate in hippocampal astrocytes treated with LPS (50 ng/mL, 3 h) alone or in presence of either increasing concentrations of minocycline (10–100 nM) or blockers of proinflammatory cytokines (IL-1 $\alpha$  and rmsTNF- $\alpha$ R1; 300 ng/mL each); right, averaged data normalized to control of Etd uptake rate in hippocampal astrocytes treated with TNF- $\alpha$ , IL-1 $\beta$ , or a mixture (MIX) of IL-1 $\beta$  and TNF- $\alpha$  (20 ng/mL each; 3 h) alone or in presence of carbenoxolone (200  $\mu$ M; MIX + CBX). Note that minocycline and cytokine blockers were applied 15 min before and all through the LPS treatment whereas CBX was applied 15 min before and during Etd uptake recordings. Data are obtained from 3 to 20 independent experiments. ### $P < 0.001$ , # $P < 0.05$ , they indicate that Etd uptake is significantly different from control condition without any treatment (signed-rank Wilcoxon test). The effect of the MIX was not significantly different than the effect of LPS alone ( $P > 0.5$ , Mann-Whitney  $U$ -test). \*\* $P < 0.01$ ; \*\*\* $P < 0.001$ , effect of minocycline (Kruskal Wallis followed by Dunn's Multiple Comparison test) or inhibitors of cytokine receptors treatments (two-tailed Mann-Whitney  $U$ -test) compared with the effect induced by LPS on Etd uptake; & $P < 0.05$ ; && $P < 0.01$ , effect of cytokines TNF- $\alpha$  and IL-1 $\beta$  and CBX compared with the effect induced by MIX on Etd uptake (two-tailed Mann-Whitney  $U$ -test).

and Suprenant, 2006), the effect of the P2X<sub>7</sub>R blocker Brilliant Blue G (BBG) was tested. BBG (1 μM), by itself, reduced the LPS-induced uptake (to 167% of the control,  $n = 8$ ) but this effect was not statistically significant compared with LPS treatment alone ( $n = 8$ , Fig. 4). In addition, the inhibition of LPS-induced Etd uptake by La<sup>3+</sup> (Fig. 4) and La<sup>3+</sup>+BBG (not shown) were not significantly different.

As the pharmacology of HCs is rather limited and does not always discriminate between Cx HCs and Panx channels (see Giaume and Theis, 2010), an alternative approach consists in using the mimetic peptides Gap26 and <sup>10</sup>Panx1, that act at the level of the first extracellular loop of Cx43 (Evans et al., 2006) and Panx1, thus blocking their hemichannel channel function, respectively (Pelegriin and Surprenant, 2006; Thompson et al., 2008; Wang et al., 2012). We observed that Gap26 (0.16 mM) blocked the membrane permeability induced by LPS treatment, while in contrast <sup>10</sup>Panx1 mimetic peptide (0.4 mM) had no significant inhibitory effect on LPS-induced Etd uptake (Fig. 4B). Finally, when both mimetic peptides Gap26 and <sup>10</sup>Panx1 were applied together, their effect was not significantly different than the effect of Gap26 alone. However, using the Mann–Whitney test to compare the data obtained for LPS treatment alone and LPS treatment in the presence of mimetic peptide <sup>10</sup>Panx1 ( $n = 20$  and 7 independent experiments, respectively), we found that they are statistically different ( $P < 0.05$ ) which further suggested the occurrence of a minor contribution of Panx1 channels. In contrast, using this former test no statistical difference ( $P > 0.05$ ) was found when comparing LPS treatment alone and in the presence of BBG ( $n = 20$  and 8 independent experiments, respectively). Altogether, these results demonstrate that, similarly to cortical cultured astrocytes (Retamal et al., 2007), LPS-induced Etd transmembrane transfer in hippocampal astrocytes in slices is mainly mediated by Cx43 HCs.

At the developmental stage when our experiments were conducted, astrocytes express both Cx43 and Cx30 (Kunzelmann et al., 1999; Nagy et al., 1999). To overpass the pharmacological approach of HC activity which is still a matter of debate (Dahl et al. 2013; Hansen et al., 2014a,b; Wang et al., 2007) and to complete the identification of the molecular nature of Cx HCs responsible for the LPS-induced Etd transmembrane transfer in astrocytes, three types of transgenic mice were used: Cx43-deficient (Cx43(fl/fl):GFAP-cre), Cx30-deficient (Cx30-/-) and double Cx43/Cx30 knock-out (Cx30-/-Cx43(fl/fl):GFAP-cre) mice (Pannasch et al., 2011; Rouach et al., 2008; Roux et al., 2011; Wallraff et al., 2006). Because unlike eGFP mice, these transgenic mice do not express any reporter molecule in astrocytes, Etd uptake was investigated in all Etd-positive cells in the stratum radiatum area adjacent to CA1 (Fig. 4C). This alternative quantification was validated as follows: (i) in the wild-type mouse (C57BL/6) most of Etd-

positive cells (87%,  $n = 121$  cells) in LPS-treated hippocampal slices were identified as astrocytes by post-fixation staining, using an anti-GFAP antibody (Fig. 4A), and (ii) when the increase in dye uptake was measured in all Etd-positive cells of LPS-treated slices derived from C57BL/6, the Etd uptake ratio was similar to that measured in GFAP-eGFP-positive astrocytes in acute slices from the corresponding reporter mice (Fig. 4C). In all cases Etd uptake was suppressed by CBX treatment.

In Cx30<sup>-/-</sup> mice, the increase in Etd uptake induced by LPS was similar to that monitored in hippocampal astrocytes derived from wild-type mice (C57BL/6 mice; Fig. 4D). In contrast, the LPS-induced Etd uptake was found to be greatly reduced in Cx43(fl/fl):GFAP-cre mice and in double Cx30-/-Cx43(fl/fl):GFAP-cre knock-out mice (Fig. 4D). Moreover, in Cx30-/- slices, the pharmacological profile of the Etd uptake showed a pattern (Fig. 4E) similar to that described in GFAP-eGFP mice (Fig. 4B). Indeed, CBX completely abolished (105% of the control;  $n = 5$ ) the LPS-evoked Etd uptake (173%,  $n = 6$ ) that was also significantly inhibited by 400 μM La<sup>3+</sup> (114% of the control,  $n = 7$ ). Moreover, as in control mice this uptake was not significantly affected by BBG (Fig. 4E). Altogether these data obtained with transgenic animals confirm that LPS-induced Etd uptake in astrocytes operates mainly through Cx43 HCs.

### **Activation of Connexin43 Hemichannels Increases Intracellular Ca<sup>2+</sup> in Hippocampal Astrocytes**

Treatment of hippocampal slices with LPS (50 ng/mL, 3 h) resulted in increased level of [Ca<sup>2+</sup>]<sub>i</sub> in astrocytes identified by SR 101 labeling (Fig. 5A) and loaded with Fluo-4/AM (Fig. 5A,B) to more than twice (232%,  $n = 176$  cells) the [Ca<sup>2+</sup>]<sub>i</sub> level monitored in control conditions ( $n = 130$  cells, Fig. 5B,C). This increase was blocked by minocycline (50 nM), confirming that the initial cell population targeted by LPS treatment is microglia (Fig. 5B,C). Furthermore, the increase of [Ca<sup>2+</sup>]<sub>i</sub> in astrocytes was also maintained to control level by treatment with the two mimetic peptides (Gap26 + <sup>10</sup>Panx1), pointing out a role for HCs activity, in addition to microglial activation (Fig. 5C). The significant differences ( $P < 0.0001$ ; *U*-test) between [Ca<sup>2+</sup>]<sub>i</sub> increases in LPS-treated slices derived from wild-type mice as compared with double knock-out (Cx30-/-Cx43(fl/fl):GFAP-cre) mice further indicates that CxHCs constitute the major component responsible for [Ca<sup>2+</sup>]<sub>i</sub> increase in LPS treated astrocytes (Fig. 5C).

Since our observations indicated that the release of IL-1β and TNF-α from activated microglia was required to activate astrocytes HC in presence of LPS (Fig. 3), we determined whether these cytokines were mediating the [Ca<sup>2+</sup>]<sub>i</sub> increase induced by LPS. When TNF-α and IL-1β (20 ng/mL each) were tested individually, they induced a significant (146%,  $n = 59$  cells and 141%,  $n = 65$  cells, respectively)

but lower increase in  $[Ca^{2+}]_i$  than LPS (232%; TNF- $\alpha$  vs. LPS and IL-1 $\beta$  vs. LPS,  $P < 0.0001$ ;  $U$ -test). Nevertheless simultaneous application of cytokines (MIX) increased Etd uptake (202%,  $n = 26$  cells) to a level similarly as that induced by LPS (MIX vs. LPS,  $P > 0.05$ ;  $U$ -test; Fig. 5D). The effect of MIX on  $[Ca^{2+}]_i$  level was prevented by the Cx43 hemichannels blocker Gap26 (102%,  $n = 35$  cells; Fig. 5D). Finally, in the presence of specific blockers of each cytokine pathways, i.e. the receptor antagonist IL-1ra and the soluble receptor sTNF- $\alpha$ R1 (300 ng/mL each), LPS no longer increased  $[Ca^{2+}]_i$  levels in hippocampal astrocytes (Fig.

5D). As all these experiments were performed in the presence of external  $Ca^{2+}$ , these observations suggest that the LPS-induced activation of microglia triggers Cx HCs activity that, in turn, allows  $Ca^{2+}$  influx in astrocytes.

### Astroglial Connexin43 Hemichannels Mediate a Decrease in the Strength of Excitatory Synaptic Transmission and an Enhancement of Glutamate Release

Astroglial connexin43 HCs are involved in the release of active molecules (i.e. gliotransmitters) that are able to

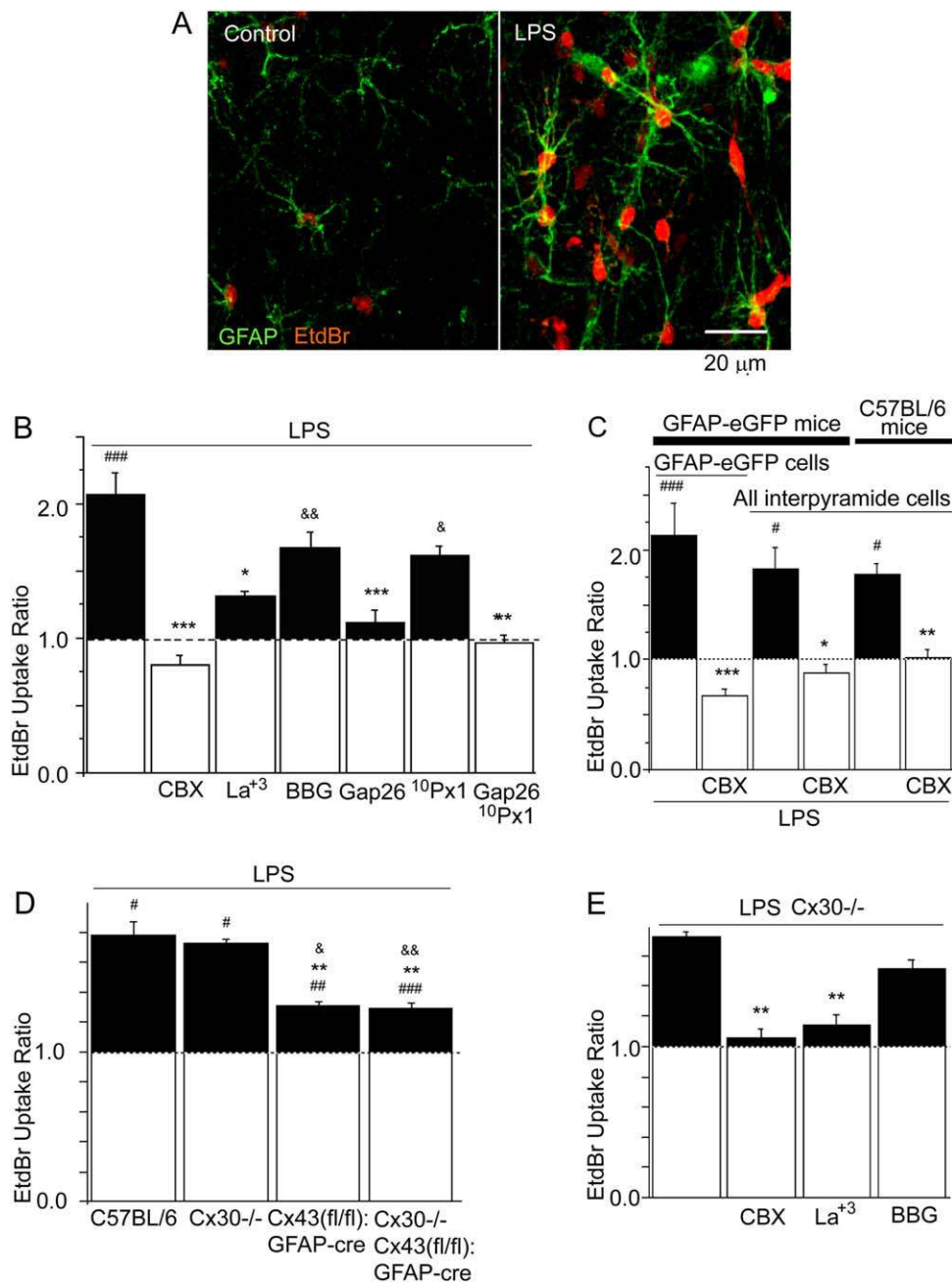


FIGURE 4: (Continued)

modulate neurotransmission (Ransom and Giaume, 2013). We thus investigated whether the LPS-induced activation of Cx43 HCs modulates hippocampal excitatory synaptic transmission. To assess the strength of synaptic transmission, we compared the size of the presynaptic fiber volley (input) to the slope of the field excitatory postsynaptic potential (fEPSP, output) in *stratum radiatum*. We found a ~50% reduction in excitatory synaptic transmission of LPS-treated slices (50 ng/mL, 3 h;  $n = 10$ ), compared with control slices ( $P < 0.05$ ,  $n = 9$ ), an effect that was completely prevented by exposing slices to the Cx43 mimetic peptide Gap26 (0.16 mM), 15 min before and during LPS exposure ( $n = 6$ ; Fig. 6A). The LPS-induced reduction of the synaptic strength was prevented by specific blockers of TNF- $\alpha$  and IL-1 $\beta$  cytokine pathways, using the receptor antagonist IL-1ra and the soluble receptor sTNF- $\alpha$ R1 (300 ng/mL each), respectively (Fig. 6B). The LPS-induced decreased synaptic transmission was also mimicked by 3 h treatment with a mixture (MIX) of TNF- $\alpha$  and IL-1 $\beta$  (20 ng/mL each;  $n = 7$ ), an effect that was prevented by Gap26 (Fig. 6C,  $n = 4$ ). Therefore, activation of astroglial Cx43 HCs by LPS treatment decreases the strength of excita-

tory synaptic transmission through the release of TNF- $\alpha$  and IL-1 $\beta$ . We discarded that decreases of the excitatory synaptic transmission reflected a progressive cell death in brain slices induced by cytokines because no change in the number of dead neurons was found between control and LPS treated slices as assessed by the ethidium homodimer-1 (Etd-1) (see Methods). Since adenosine derived from astroglial ATP is known to decrease excitatory synaptic transmission through presynaptic adenosine A1 receptors (A1Rs; Pascual et al., 2005), we also tested whether A1Rs were involved in the LPS-induced effect. However, we found that inhibition of A1Rs by 8-cyclopentyl-1,3-dipropylxanthine (DPCPX, 200 nM) had a similar effect on excitatory transmission from control and LPS-treated slices (i.e. an increase of evoked fEPSP: control:  $53 \pm 23$  %,  $n = 5$ ; LPS:  $61 \pm 19$  %,  $n = 7$ ). These data indicate that the regulation of synaptic transmission by LPS-induced HC activation in astrocytes does not involve the activation of A1Rs.

Another plausible mechanism would be that LPS induces glutamate release and thereby decreases excitatory synaptic transmission via activation of extrasynaptic glutamate

**FIGURE 4: LPS-induced astrocyte membrane permeabilization occurs mainly through Cx43 hemichannels.** (A) Fluorescence images of astrocytes of acute hippocampal slices derived from non-transgenic C57BL/6 (WT) mice showing Etd uptake (red) under control conditions (Control) and under LPS (50 ng/mL, 3 h) exposure (LPS). After the experiments, post-fixation immunochemistry allowed to identify GFAP-labeled (green) astrocytes. (B) Averaged data normalized to control (dashed line) of the Etd uptake rate in hippocampal astrocytes treated with LPS (50 ng/mL, 3 h) alone or in presence of the HCs blockers: CBX (200  $\mu$ M), La<sup>+3</sup> (400  $\mu$ M) and Gap26 (0.16 mM), the P<sub>x1</sub> channel blocker <sup>10</sup>Px1 (0.4 mM), the P<sub>2X<sub>7</sub></sub> blocker BBG (1  $\mu$ M) or a mixture of blockers, applied 15 min before and during Etd measurements. Data are obtained from 5 to 20 independent experiments. \* $P < 0.05$ ; \*\*\* $P < 0.001$ : effects of blockers compared with the effect induced by LPS alone on Etd uptake; & $P < 0.05$ ; && $P < 0.01$ : effects of blockers (BBG and <sup>10</sup>Px1) compared with LPS/CBX treatment effect (Kruskal-Wallis test followed by Dunn's Multiple Comparison *post hoc* test). The effect of LPS/CBX treatment is not significantly different from LPS/La<sup>+3</sup>, LPS/Gap26, or LPS/Gap26/<sup>10</sup>Px1 treatments while LPS/BBG and LPS/<sup>10</sup>Px1 are statistically different from LPS/CBX treatment effect. Note that when compared with control condition (without LPS), Etd uptake is increased by LPS treatment ( $P < 0.001$ , Wilcoxon signed-rank test), even in presence of BBG ( $P < 0.01$ ) and <sup>10</sup>Px1 ( $P < 0.05$ ; Wilcoxon signed-rank test). On the contrary, LPS does not induce any Etd uptake increase in presence of CBX, Gap26, or Gap26/<sup>10</sup>Px1 compared with control condition ( $P > 0.05$ , Wilcoxon signed-rank test). (C) Averaged data normalized to control (dashed line) of the Etd uptake rate of hippocampal astrocytes treated with LPS (50 ng/mL, 3 h) alone or in presence of carbenoxolone (CBX, 200  $\mu$ M) in acute slices derived from either transgenic GFAP-eGFP or non-transgenic C57BL/6 mice. Note that for the analysis, Etd uptake was measured in GFAP-eGFP cells uniquely from transgenic mice or in all cells positive for Etd from both transgenic GFAP-eGFP and nontransgenic C57BL/6 mice. Data are obtained from 3 to 20 independent experiments. # $P < 0.05$ ; ### $P < 0.001$ : Etd uptake is increased by LPS treatment compared with control condition (Wilcoxon signed-rank test); \* $P < 0.05$ ; \*\* $P < 0.01$ ; \*\*\* $P < 0.001$ : effect of CBX compared with the effect induced by LPS alone on Etd uptake (two-tailed Mann-Whitney *U*-test). (D) Comparison of Etd uptake in LPS-treated astrocytes of acute hippocampal slices derived from non-transgenic C57BL/6, and for transgenic Cx30-deficient (Cx30<sup>-/-</sup>), Cx43-deficient (Cx43(fl/fl):GFAP-cre) and double Cx30/Cx43-deficient (Cx30<sup>-/-</sup>Cx43(fl/fl):GFAP-cre) mice. Averaged data normalized to Etd uptake obtained in control condition (without LPS, dashed line) for the corresponding mouse line. Data are obtained from 6 to 11 independent experiments. # $P < 0.05$ , ### $P < 0.01$ , ### $P < 0.001$ : LPS vs. control \*\* $P < 0.01$ : LPS-induced Etd uptake in knock-out mice compared with C57BL/6 mice. & $P < 0.05$ ; && $P < 0.01$ : comparison with LPS-induced Etd uptake in Cx30<sup>-/-</sup> mice. Note that no significant effect is observed between LPS-induced Etd uptake in Cx43-deficient and double Cx30/Cx43-deficient mice (Kruskal-Wallis test followed by Dunn's Multiple Comparison *post hoc* test). In addition, LPS induces a significant increase in Etd uptake as compared with control condition in all genotypes tested ( $P < 0.05$ ; Wilcoxon signed-rank test). However, this increase is significantly larger in WT and Cx30<sup>-/-</sup> mice compared with Cx43-deficient and double Cx30/Cx43-deficient mice (interaction:  $P < 0.05$ ; two-way ANOVA, mixed model). (E) Averaged data normalized to control (dashed line) of the Etd uptake rate in astrocytes of acute hippocampal slices derived from Cx30-deficient (Cx30<sup>-/-</sup>) mice treated with LPS (50 ng/mL, 3 h) alone or in presence of carbenoxolone (CBX, 200  $\mu$ M), the Cx HC blocker La<sup>3+</sup> (400  $\mu$ M) and the P<sub>2X<sub>7</sub></sub> blocker BBG (1  $\mu$ M). Data are obtained from four to seven independent experiments. \* $P < 0.05$ ; effect of different blockers compared with the effect induced by LPS alone on Etd uptake (Kruskal-Wallis test followed by Dunn's Multiple Comparison *post hoc* test). Note that there is no significant difference between LPS-induced Etd uptake in presence of CBX or La<sup>3+</sup>. Moreover, compared with control condition (without LPS), Etd uptake is increased by LPS treatment, even in presence of BBG but not in presence of CBX or La<sup>3+</sup> ( $P > 0.05$ , Wilcoxon signed-rank test). Note that blockers (B–D) were applied 15 min before and during Etd measurements.

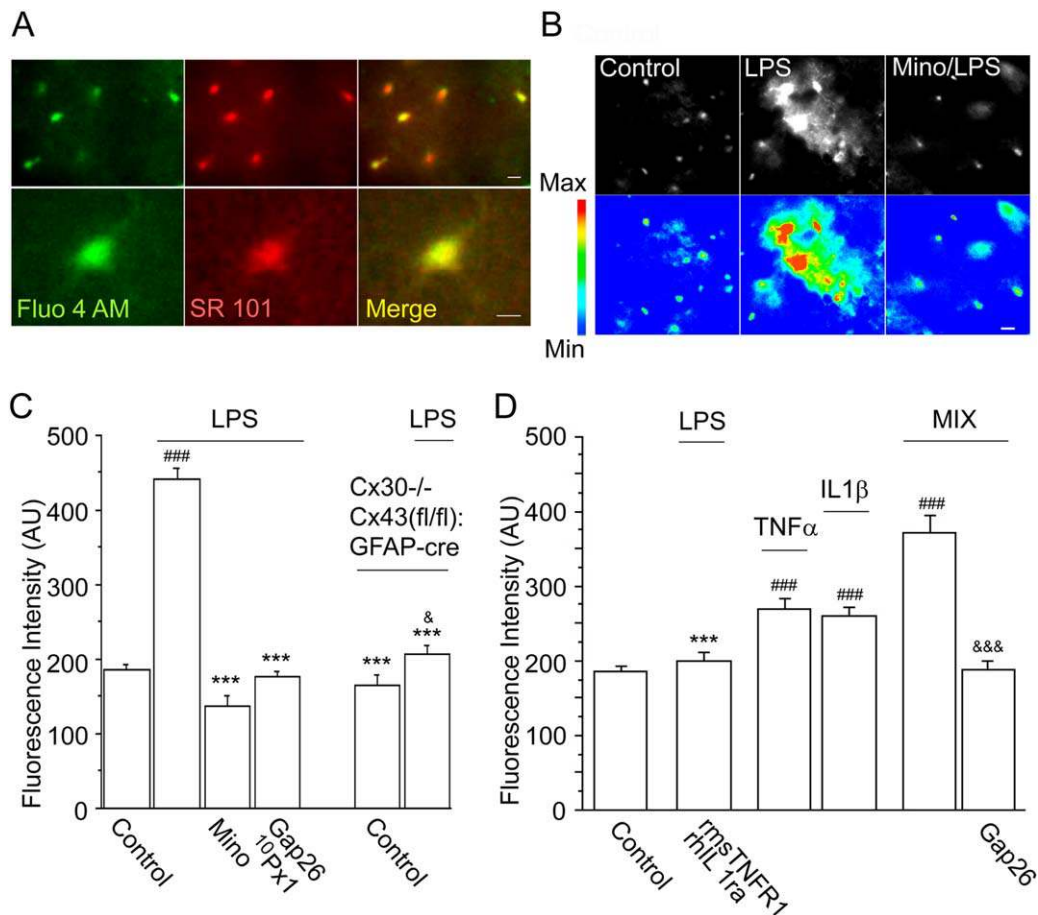


**FIGURE 5: Activated Cx43 hemichannels allow calcium influx into astrocytes in acute LPS-treated hippocampal slices.** (A) Fluorescent images of astrocytes from acute hippocampal slices derived from nontransgenic C57BL/6 (WT) mice preloaded with Fluo 4/AM (4  $\mu$ M; green, left panels) and labeled with SR 101 (1  $\mu$ M; red, middle panels) at low (upper panels, scale bar 20  $\mu$ m) and high (lower panels, scale bar 10  $\mu$ m) magnification were superimposed to demonstrate the colocalization between Fluo 4/AM and SR 101 stainings (yellow, right panels). (B) Pseudocolored images in astrocytes from acute hippocampal slices derived from nontransgenic C57BL/6 (WT) mice representative of  $[Ca^{2+}]_i$  levels under control conditions (control), and treated with LPS (50 ng/mL, 3 h) alone (LPS) or in presence of 50 nM minocycline (Mino/LPS) applied 15 min before and all through the LPS treatment. Slices were preloaded with Fluo-4/AM before treatments. Scale bar, 10  $\mu$ m. (C) Left, averaged data of fluorescence levels in arbitrary units (AU) in astrocytes from Fluo-4/AM preloaded slices derived from nontransgenic C57BL/6 (WT) mice under control conditions, and treated with LPS (50 ng/mL, 3 h) alone or in presence of minocycline (50 nM), and Gap26 (0.16 mM) plus  $^{10}$ Panx1 (0.4 mM) applied 15 min before and all through the LPS treatment. Right, averaged data of fluorescence levels in arbitrary units (AU) in astrocytes from Fluo-4/AM preloaded slices derived from transgenic (Cx30(-/-)Cx43(fl/fl):GFAP-cre) mice under control conditions and treated with LPS (50 ng/mL, 3 h). Data are obtained from at least three independent experiments with a number of cells ranging from 39 to 179. In WT mice, among all tested treatments, only LPS significantly increases  $[Ca^{2+}]_i$  compared with control (### $P < 0.001$ ). \*\*\* $P < 0.001$ , comparison with the effect induced by LPS alone on Etd uptake (Kruskal-Wallis test followed by Dunn's Multiple Comparison test). No difference in the basal  $[Ca^{2+}]_i$  level is observed between astrocytes from WT and Cx30(-/-)Cx43(fl/fl):GFAP-cre mice (two-tailed Mann-Whitney *U*-test). However, LPS effect on  $[Ca^{2+}]_i$  level is significantly different in these two genotypes since it only induces a slight increase in Cx30(-/-)Cx43(fl/fl):GFAP-cre astrocytes (& $P < 0.05$ , Mann-Whitney *U*-test) compared with WT ( $P < 0.001$ , two-way ANOVA). (D) Averaged data of fluorescence levels in arbitrary units (AU) in astrocytes from Fluo-4/AM preloaded slices derived from non-transgenic C57BL/6 (WT) mice under control conditions, treated with LPS (50 ng/mL, 3 h) in presence of blockers of proinflammatory cytokines (IL-1ra and rmsTNF- $\alpha$ R1; 300 ng/mL each) applied 15 min before and all through the LPS treatment and treated with proinflammatory cytokines TNF- $\alpha$  (20 ng/mL; 3 h) or IL-1 $\beta$  (20 ng/mL; 3 h), or with a mixture (MIX) of both alone or in presence of Gap26 (0.16 mM; MIX+Gap26) applied 15 min before and all through the MIX treatment. Data are obtained from at least 3 independent experiments with a number of cells ranging from 26 to 125. \*\*\* $P < 0.001$ , comparison of the effect of LPS in WT mice in presence of inhibitors of cytokines (IL-1ra and sTNF- $\alpha$ R1; 300 ng/mL each) with the effect induced by LPS alone on  $Ca^{2+}$  levels (two-tailed Mann-Whitney *U*-test). Treatments with cytokines, TNF- $\alpha$  (20 ng/mL; 3 h), IL-1 $\beta$  (20 ng/mL; 3 h), or a mixture (MIX) of both significantly increase intracellular  $Ca^{2+}$  compared with control (### $P < 0.001$ ) but the effect of MIX is significantly larger than the effect of TNF- $\alpha$  ( $P < 0.001$ , two-tailed Mann-Whitney *U*-test) and from the effect IL-1 $\beta$  ( $P < 0.001$ , two-tailed Mann-Whitney *U*-test) applied alone. The increase in  $Ca^{2+}$  levels by MIX is totally prevented by the hemichannel blocker Gap26 (0.16 mM; &&& $P < 0.001$ , two-tailed Mann-Whitney *U*-test).

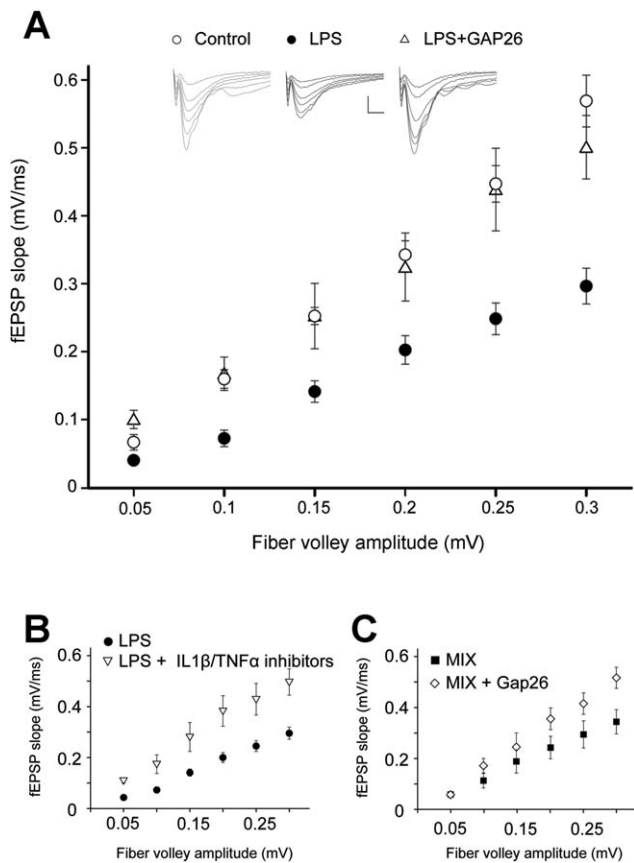


**FIGURE 6: LPS inhibits excitatory synaptic activity via the activation of Cx43 hemichannels.** (A) Basal synaptic transmission in hippocampal slices. Input/output curve is reduced by 50% in LPS-treated acute hippocampal slices ( $P \leq 0.05$ , LPS), an effect inhibited by pretreatment of slices with the Cx43 hemichannel blocker Gap26 (160  $\mu\text{M}$ ;  $P \leq 0.05$ , LPS + Gap26), (B) as well as pretreatment with the cytokine (TNF $\alpha$  and IL1 $\beta$ ) inhibitors IL-1ra and sTNF- $\alpha$ R1 ( $P \leq 0.05$ , LPS + inhibitors). (C) Conversely, treatment of slices with both TNF $\alpha$  and IL1 $\beta$  (Mix) mimics the LPS effect ( $P \leq 0.05$ , Mix) and is also prevented by pre-incubation with Gap26 ( $P \leq 0.05$ , Mix + Gap26) Scale bar, 0.25 mV, 5 ms.

receptors. To strengthen this statement, we treated hippocampal slices with LPS (50 ng/mL) for 0, 60, and 180 min to assess extracellular L-glutamate levels ( $n = 4$  for each assay unless indicated). In control conditions (i.e. in the absence of LPS), the level of L-glutamate gradually increased over these time points, and this trend was amplified by LPS treatment (50 ng/mL, 3 h); at 60 min LPS and MIX treatments induced a slight but not significant increase in the level of L-glutamate (Fig. 7A); however, after 180 min, LPS treatment significantly impacted the level of L-glutamate which showed a  $239 \pm 22\%$  increase ( $n = 4$ ). In addition, the LPS-induced increase in L-glutamate was significantly reduced by minocycline ( $159 \pm 47\%$ ,  $n = 4$ ) and prevented by the cocktail of the two cytokine receptor antagonists, IL-1ra and the soluble receptor sTNF- $\alpha$ R1 (300 ng/mL each;  $113 \pm 32\%$ ,  $n = 5$ ).

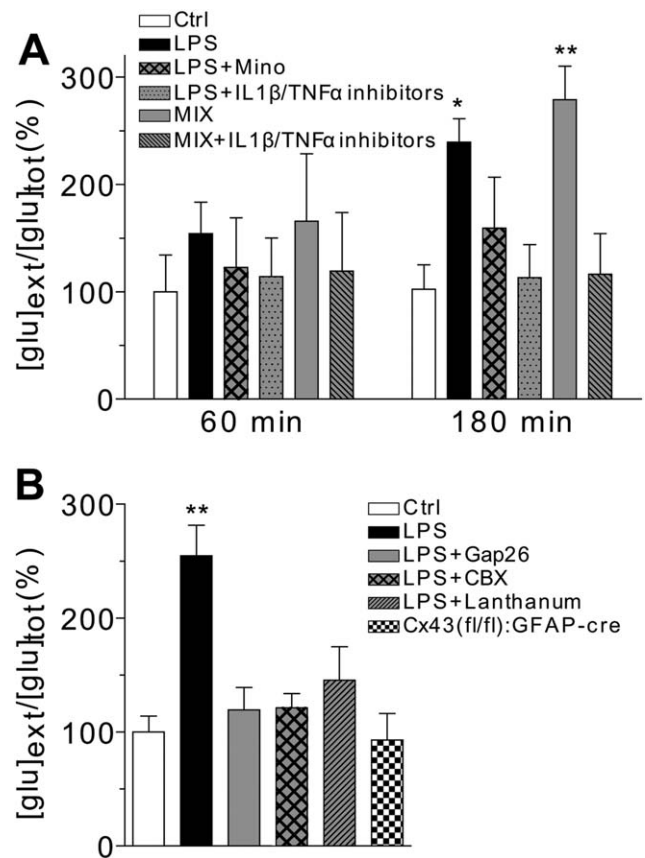


**FIGURE 7: LPS treatment increases extracellular levels of glutamate via the activation of Cx43 hemichannels.** (A) Cx43-dependent LPS-induced increase in the released fraction of L-glutamate in hippocampal slices. L-glutamate levels were resolved from NDA derivatized samples of extracellular medium, analyzed by CE-LIF. LPS does not increase L-glutamate level after 60 min treatment gradually but its effect becomes significant at 180 min ( $P < 0.05$ ). Note that this feature is mimicked by treatment with both the TNF- $\alpha$  and IL-1 $\beta$  (MIX;  $P < 0.01$ ). Conversely, the potentiating effect of LPS (180 min) was inhibited by minocycline (Mino) and was prevented by pretreating the slices with rmsTNFR1 and rhIL1ra. The effect of TNF- $\alpha$  and IL1 $\beta$  (MIX, 180 min) is prevented when pretreating the slices with the rmsTNFR1 and rhIL1ra ( $P < 0.01$ ). (B) In wild-type mice, the LPS-induced increase in L-glutamate released fraction ( $P < 0.01$ ) measured at 180 min is fully prevented by carbenoxolone (CBX), or by specific inhibition of Cx43 with Gap26 or lanthanum. Similarly, LPS treatment does not increase L-glutamate level measured at 180 min in Cx43-deficient mice (Cx43(fl/fl):GFAP-cre mice). Statistical analysis: ANOVA followed by Newman-Keuls Multiple comparison test,  $*P < 0.05$   $**P < 0.01$  as compared with control conditions. Represented data are means  $\pm$  SEM for  $n = 4$  independent measurements made in duplicate. Note that in this figure data are normalized to control values and that fraction of L-glutamate released in control situation are 0.006614 and 0.02655 nmol/mg prot in A and B, respectively.

As a complement of these observations, L-glutamate level was increased by 180 min treatment with the MIX of the two proinflammatory cytokines ( $279 \pm 31\%$ ,  $n = 5$ ), an effect that again was prevented by the two receptor antagonists

( $116 \pm 37\%$ ,  $n = 5$ ; Fig. 7A). Moreover, pharmacological inhibition of HCs channels activation with CBX reversed the effect of LPS on L-glutamate level to  $121 \pm 13\%$  ( $n = 4$ ) at 180 min ( $P > 0.05$  vs. control) suggesting that the release of L-glutamate induced by LPS operates mainly through HCs. Interestingly, CBX did not affect the basal levels of L-glutamate over the 3 h period in absence of LPS. To assess more specifically the contribution of Cx43 HCs, hippocampal slices were treated with either Gap26 or  $\text{La}^{3+}$ . As shown in Fig. 7B, Gap26 (0.16 mM) reversed the effect of LPS and fully mimicked the action of CBX on glutamate levels ( $119 \pm 19\%$ ,  $n = 4$ ) suggesting a major contribution of Cx43 HCs to the release of glutamate induced by LPS. When slices were treated with  $\text{La}^{3+}$  that blocks Cx HCs, but not Panx1 channels, LPS-induced release of glutamate over the time course was reduced to a similar extent than under Gap26 or CBX (Fig. 7B). Indeed, level of L-glutamate under  $\text{La}^{3+}$  was  $145 \pm 29\%$  ( $n = 4$ ) of controls values at 180 min. Once again, these results point out a major contribution for Cx43 HCs. To complement this pharmacological study we also investigated the role of Cx43 HCs in driving the release of L-glutamate by using acute hippocampal slices from Cx43-deficient (Cx43(fl/fl):GFAP-cre) mice treated with LPS. Consistent with our observations with CBX,  $\text{La}^{3+}$ , and Gap26 the release of L-glutamate monitored at 180 min was reduced to  $93 \pm 23\%$  ( $n = 4$ ) in glial conditional Cx43 KO mice compared with wild-type mice (Fig. 7B). In conclusion, under LPS-treatment, glutamate increases extracellularly, an effect that requires the activity of astroglial Cx43 HCs.

## Discussion

In the present work, we investigated the effects of the inflammatory agent LPS on astrocyte HC activity, on GJC-mediated communication in acute hippocampal slices and the functional consequences of astrocyte HC opening on astrocyte calcium levels, glutamate release and synaptic activity of pyramidal CA1 neurons. We found that LPS (50 ng/mL, 3 h) activates HCs in hippocampal astrocytes, while no change is observed in astroglial GJC-mediated dye coupling. These effects require primarily a microglial activation and the resulting release of at least two identified proinflammatory cytokines, IL-1 $\beta$  and TNF- $\alpha$ . Moreover, we observed that LPS increases  $[\text{Ca}^{2+}]_i$  levels in astrocytes, an effect that results from the activation of astroglial HCs. An important consequence of this HC activation in astrocytes is a strong reduction ( $\approx 50\%$ ) of basal excitatory activity of CA1 hippocampal neurons that is associated with an enhanced glutamate release in the extracellular space.

Astrocytes express two main Cxs, i.e., Cx43 and Cx30, that provide the molecular constituents to the LPS-induced HC activity in astrocytes reported here. In addition, Panx-1

channels could have also been involved in this process as indicated previously (Garré et al., 2010; Iglesias et al., 2009; Karpuk et al., 2011; Suadicani et al., 2012). To discriminate which of these three molecular candidates is involved in the LPS-induced uptake in astrocytes we used a combination of pharmacological and genetic tools (Giaume and Theis, 2010). From the pharmacological approach, we found that CBX totally abolishes the Etd transmembrane transfer in eGFP-GFAP-positive cells indicating that astroglial HCs contribute to the LPS-induced Etd uptake. The strong effects of  $\text{La}^{3+}$  and Gap26 indicate that Cx HCs are mainly involved in this phenomenon. Since their impact does not differ from that of CBX, which affects both Cx and Panx1 HCs, we concluded that Panx1 channels are not a major actor involved in the response of astrocytes to LPS treatment. However, a weak but statistically significant effect of the mimetic peptide  $^{10}\text{P}x1$  on the LPS-induced Etd uptake (see Fig. 4B) outlines the occurrence of a minor pannexin-dependent component. Moreover, the use of transgenic knock-out mice allowed discriminating between Cx43 and Cx30 HCs. Because LPS has a similar effect in Cx30 $^{-/-}$  and wild-type mice, we concluded that Cx30 HCs seem not to be involved. In contrast, in Cx43(fl/fl):GFAP-cre mice, the Etd uptake triggered by LPS treatment is suppressed, which evidences the key role of astroglial Cx43 the LPS-induced Etd uptake. Accordingly, LPS-induced Etd uptake is similarly reduced by  $\text{La}^{3+}$  in wild-type slices and removal of Cx43 in Cx43(fl/fl):GFAP-cre slices. Finally, we observed that Cx43 HCs activated by LPS treatment of acute hippocampal slices provide a pathway for glutamate release. This finding constracts the recent report claiming that Cx43 HCs are not permeable to glutamate when using the Cx43-expressing *Xenopus laevis* system and a free calcium solution treatment to activate HCs (Hansen et al., 2014b). However, the systems way used to activate HCs, are so different compared to the present study that it is difficult to compare the two situations and make a conclusive statement.

The effect of minocycline preventing the increase of dye uptake and of  $[\text{Ca}^{2+}]_i$  in astrocytes, as well as the release of glutamate, demonstrates that LPS treatment initially targets microglial cells. This observation is in agreement with their role as inflammation sensors in the central nervous system when LPS is used as a trigger of neuroinflammation (Block et al., 2007; see also Retamal et al., 2007). As a secondary step, the release of TNF- $\alpha$  and IL-1 $\beta$  from LPS-activated microglia targets astrocytes where Cx43 HC opening takes place as already observed in astrocytes cultured with microglia (Même et al., 2006; Retamal et al., 2007). In hippocampal slices this effect, as well as the increase in  $[\text{Ca}^{2+}]_i$  and the release of glutamate, is also mediated by the release of these two proinflammatory cytokines from microglia, since treatment with the receptor antagonist IL-1ra and the soluble

receptor sTNF- $\alpha$ R1 prevents the effect of LPS on Cx43 HCs and a MIX of the two cytokines mimics it. In a previous study performed using co-cultures of astrocytes and microglia, we found that the selective stimulation of microglia with LPS induces an opposite regulation of Cx43 channel functions, i.e. an inhibition of GJC and an activation of Cx43 HCs in astrocytes (Retamal et al., 2007). In the present work performed *ex vivo*, we observed that LPS stimulation of microglia induces the activation of HCs in astrocytes while there is no change in GJC properties. The lack of LPS-induced uncoupling was not attributed to Cx30-based GJCs, the second astroglial Cx which is not expressed in primary culture (Kunzelmann et al., 1999), indeed in the Cx30 KO LPS treatment was still ineffective on gap junctional communication. In a previous work we suggested that in cultured astrocytes p38 activation affects Cx43 forming hemichannel activity through NO production and changes in their redox potential. Moreover, we hypothesized that p38 activation possibly affects Cx43 forming gap junction channels through changes in their phosphorylation state unrelated to shifts in electrophoretic mobility or oxidation modifications of Cx43 (Retamal et al., 2007). These statements implicated that the regulatory pathways of the two channel functions of Cx43 are not necessarily linked which could explain the discrepancy observed between our *in vitro* and *ex vivo* approaches, but the dissection of these regulatory pathways was not under the scope of the present study and this hypothesis remains to be studied.

Importantly, opening of astroglial Cx43 HCs, induced by LPS (50 ng/mL; 3 h) reduces basal excitatory synaptic transmission. This result contrasts with the recently reported short-term effect of LPS (<5 min), applied at higher concentration (500 ng/mL), which induces a rapid and transient increase in the frequency of spontaneous AMPAR-mediated excitatory currents (Pascual et al., 2012). This short-term effect of LPS was attributed to an astroglial release of glutamate activating neuronal mGluR5 receptors (Pascual et al., 2012). These distinct effects of LPS treatment could be attributed to the different concentrations and time scales of LPS application, engaging distinct downstream pathways following release of different levels of glutamate, which can differentially regulate synaptic activity. Indeed, according to the magnitude and spatiotemporal patterns of gliotransmitter release, as well as the type and proximity of neuronal receptors targeted, a same gliotransmitter can induce differential regulations of neurotransmission (see Araque et al., 2014).

In pathological conditions, Cx43 HCs are well known to release ATP (Thompson and MacVicar, 2008), a gliotransmitter rapidly metabolized by ectonucleotidases into adenosine, which strongly decreases presynaptic release probability (Pascual et al., 2005; but see Lovatt et al., 2012). We also

observed that a 3 h LPS treatment increases  $[Ca^{2+}]_i$  in astrocytes and extracellular ATP levels, both increases being dependent on Cx43 HCs activity (data not shown). However, the LPS-mediated depression of glutamatergic synaptic activity does not result from an increase in the activation of adenosine A1 receptors, as indicated by the lack of differential effect of the A1 receptor antagonist DPCPX in control and LPS conditions. Alternatively, we cannot exclude that inflammatory cytokines, such as IL1 $\beta$ , directly contributes to the LPS-induced depression of excitatory synaptic transmission, since they have already been reported to decrease glutamatergic synaptic activity in the hippocampus (Murray et al., 1997; Yang et al., 2005;), in contrast to other cytokines such as TNF- $\alpha$  (Beattie et al., 2002). However, this hypothesis may not be prominent since we observed that the LPS-induced inhibition of glutamatergic transmission is prevented by the Cx43 HC blocker Gap26 indicating an astrocyte contribution step, as Cx43 is not expressed in postnatal neurons (Condorelli et al., 2003; Theis et al., 2003). Interestingly, a recent study performed in the spinal cord indicates that, there also, the induction of both synaptic LTP and hyperalgesia by TNF- $\alpha$  and IL-1 $\beta$  are not direct neuronal effect, as currently thought (Kawasaki et al., 2008; Park et al., 2011; Zhang et al., 2011), but are mediated indirectly via the activation of spinal glial cells (Gruber-Schoffnegger et al., 2013). Although the kinetics and the molecular mechanisms involved in the effect of the two cytokines are likely different in the spinal cord and the hippocampus, this study and ours point out the role of glia in the TNF- $\alpha$ - and IL-1 $\beta$ -mediated contribution to the control of neurotransmission. Interestingly, we also showed that the LPS-induced Cx43 HC activation in astrocytes strongly increases extracellular glutamate levels. Although a recent study also suggested that LPS induces astroglial glutamate release (Pascual et al., 2012), this effect was transient due to the short application of LPS, and most likely resulted in a smaller extracellular build up of glutamate compared with our study. The LPS effect on extracellular glutamate levels may be mediated by TNF- $\alpha$ , which is well known to induce astroglial release of glutamate (see Santello et al., 2011). In our conditions, glutamate released by astrocytes over prolonged time periods likely act on perisynaptic and extrasynaptic glutamate receptors, such as metabotropic receptors (mGluRs; Lujan et al., 1996) known to depress excitatory synaptic transmission at the Schaffer collateral-CA1 synapse via changes in release probability (Overstreet et al., 1997). Alternatively, other mechanisms related to the prolonged increase in extracellular glutamate levels may contribute to the glutamatergic synaptic depression reported here. Indeed, excess in extracellular glutamate levels induced by LPS may desensitize postsynaptic AMPARs. Additionally, strong activation of neuronal glutamatergic receptors may

lead to a massive build-up in extracellular potassium levels and subsequent neuronal depolarization (Poolos et al., 1987). *Per se*, the impairment of ion gradients and associated neuronal depolarization are expected to inhibit all ion gradient-dependent transporters and voltage-gated channels that may directly perturb action potential generation and thus underlie the synaptic depression induced by LPS. Thus multiple mechanisms related to the increase in extracellular glutamate levels may contribute to the regulation of synaptic transmission in pathological situations characterized by a glial inflammatory response. Finally, the finding that during the LPS-induced microglial activation Cx43 HC activity has a direct consequence on synaptic strength and extracellular glutamate levels outlines that the activation of Cx43 HCs in astrocytes may represent a key element of the glial response during neuroinflammation. Indeed, we found that blockade of astroglial Cx43 HCs by Gap26 is able to restore the excitatory synaptic transmission of pyramidal neurons in response to Schaffer's collaterals stimulation to control levels and to prevent the LPS-induced increase in extracellular glutamate levels. Such dynamic neuroglial interaction strengthens previous reports establishing the critical role of astrocytes in the regulation of synaptic transmission (Perea and Araque, 2010; Volterra and Steinhauser, 2004) especially in an inflammatory context (Parpura et al., 2012; Pascual et al., 2012; Santello and Volterra, 2012).

The initial microglial response followed by astroglial activation plays a central role in neuroinflammation, a process common to most brain diseases that in fine impairs neuronal activity and survival. As microglial activation and alteration of neurotransmission are two early symptoms of most brain pathologies, this work provides a basis to further understand neuronal dysfunction in brain diseases. Accordingly, the present demonstration of a sequential activation of glial cells, that includes astrocytes Cx43 HC function, should contribute to identify novel pharmacological strategies to protect neurons from exacerbated excitotoxicity during neuroinflammation.

## Acknowledgment

Grant sponsor: Caisse de Retraite et de Prévoyance des Clercs et Employés de Notaires (CRPCEN), Ligue Européenne Contre la Maladie d'Alzheimer and France Alzheimer (LECMA) (to C.G.), International Brain Organization (IBRO), Collège de France (Paris, France), Comisión Sectorial de Investigación Científica de la Universidad de la República Oriental del Uruguay (CSIC, UDELAR), and Facultad de Medicina de la Universidad de la República Oriental del Uruguay (to V.A.), CNRS, INSERM, Conseil Régional d'Aquitaine and the Agence Nationale de la Recherche (ANR) (to J.P.M.), ANR, City of Paris and Fédération pour

la Recherche sur le Cerveau (FRC) (to N.R.), and Labex Memolife (to G.D.).

The authors are grateful to the INSERM Unit U862 and Dr. Stephane Oliet for the use of the Plateforme de Chimie Analytique at the Neurocentre Magendie in Bordeaux. The authors thank Pascal Ezan for excellent technical assistance, Dr. Annette Koulakoff for helpful discussion during the work, Jérémie Teillon (Unité de Microscopie Confocale du Collège de France) for helpful contribution to the setting of the analysis of hemichannel activity, and Dr. Michael V. Bennett for reading the manuscript and providing helpful comments.

## References

- Araque A, Carmignoto G, Haydon PG, Oliet SH, Robitaille R, Volterra A. 2014. Gliotransmitters travel in time and space. *Neuron* 81:728–739.
- Araque A, Parpura V, Sanzgiri RP, Haydon PG. 1999. Tripartite synapses: Glia, the unacknowledged partner. *Trends Neurosci* 22:208–215.
- Beattie MS, Hermann GE, Rogers RC, Bresnahan JC. 2002. Cell death in models of spinal cord injury. *Prog Brain Res* 137:37–47.
- Bennett MV, Contreras JE, Bukauskas FF, Sáez JC. 2003. New roles for astrocytes: Gap junction hemichannels have something to communicate. *Trends Neurosci* 26:610–617.
- Bessis A, Béchade C, Bernard D, Roumier A. 2007. Microglial control of neuronal death and synaptic properties. *Glia* 55:233–238.
- Block ML, Zecca L, Hong JS. 2007. Microglia-mediated neurotoxicity: Uncovering the molecular mechanisms. *Nat Rev Neurosci* 8:57–69.
- Bruzzone R, Barbe MT, Jakob NJ, Monyer H. 2005. Pharmacological properties of homomeric and heteromeric pannexin hemichannels expressed in *Xenopus* oocytes. *J Neurochem* 92:1033–1043.
- Chever O, Lee CY, Rouach N. (2014) Astroglial connexin43 hemichannels tune basal excitatory synaptic transmission. *J Neurosci* 34:11228–11232.
- Condorelli DF, Trovato-Salinaro A, Mudò G, Miron MB, Belluardo N. 2003. Cellular expression of connexins in the rat brain: Neuronal localization, effects of kainate-induced seizures and expression in apoptotic neuronal cells. *Eur J Neurosci* 18:1807–1827.
- Dahl G, Qiu F, Wang J. 2013. The bizarre pharmacology of the ATP release channel pannexin1. *Neuropharmacology* 75:583–593.
- Evans WH, De Vuyst E, Leybaert L. 2006. The gap junction cellular internet: Connexin hemichannels enter the signalling limelight. *Biochem J* 397:1–14.
- Fossat P, Turpin FR, Sacchi S, Dulong J, Shi T, Rivet JM, Sweedler JV, Pollegioni L, Millan MJ, Oliet SH, Mothet JP. 2012. Glial D-serine gates NMDA receptors at excitatory synapses in prefrontal cortex. *Cereb Cortex* 22:595–606.
- Froger N, Orellana JA, Calvo CF, Amigou E, Kozoriz MG, Naus CC, Sáez JC, Giaume C. 2010. Inhibition of cytokine-induced connexin43 hemichannel activity in astrocytes is neuroprotective. *Mol Cell Neurosci* 45:37–46.
- Garré JM, Retamal MA, Cassina P, Barbeito L, Bukauskas FF, Sáez JC, Bennett MV, Abudara V. 2010. FGF-1 induces ATP release from spinal astrocytes in culture and opens pannexin and connexin hemichannels. *Proc Natl Acad Sci USA* 107:22659–22664.
- Giaume C, Kirchhoff F, Matute C, Reichenbach A, Verkhratsky A. 2007. Glia: The fulcrum of brain diseases. *Cell Death Differ* 14:1324–1335.
- Giaume C, Koulakoff A, Roux L, Holcman D, Rouach N. 2010. Astroglial networks: a step further in neuroglial and gliovascular interactions. *Nat Rev Neurosci* 11:87–99.

- Giaume C, Leybaert L, Naus CC, Sáez JC. 2013. Connexin and pannexin hemichannels in brain glial cells: properties, pharmacology, and roles. *Front Pharmacol* 4:88.
- Giaume C, Orellana JA, Abudara V, Sáez JC. 2012. Connexin-based channels in astrocytes: how to study their properties. *Methods Mol Biol* 814:283–303.
- Giaume C, Theis M. 2010. Pharmacological and genetic approaches to study connexin-mediated channels in glial cells of the central nervous system. *Brain Res Rev* 63:160–176.
- Giulian D, Baker TJ, Shih LC, Lachman LB. 1986. Interleukin 1 of the central nervous system is produced by ameboid microglia. *J Exp Med* 164:594–604.
- Gosejacob D, Dublin P, Bedner P, Hüttmann K, Zhang J, Tress O, Willecke K, Pfrieger F, Steinhäuser C, Theis M. 2011. Role of astroglial connexin30 in hippocampal gap junction coupling. *Glia* 59:511–519.
- Gruber-Schoffnegger D, Drdla-Schutting R, Hönigsperger C, Wunderbaldinger G, Gassner M, Sandkühler J. 2013. Induction of thermal hyperalgesia and synaptic long-term potentiation in the spinal cord lamina I by TNF- $\alpha$  and IL-1 $\beta$  is mediated by glial cells. *J Neurosci* 33:6540–6551.
- Hanisch UK, Kettenmann H. 2007. Microglia: active sensor and versatile effector cells in the normal and pathologic brain. *Nat Neurosci* 10:1387–1394.
- Hansen DB, Braunstein TH, Nielsen MS, MacAulay N. 2014a. Distinct permeation profiles of the connexin 30 and 43 hemichannels. *FEBS Lett* 588:1446–1457.
- Hansen DB, Ye ZC, Calloe K, Braunstein TH, Hofgaard JP, Ransom BR, Nielsen MS, MacAulay N. 2014b. Activation, permeability, and inhibition of astrocytic and neuronal large pore (hemi)channels. *J Biol Chem* 289:26058–26073.
- Hirase H, Qian L, Barthó P, Buzsáki G. 2004. Calcium dynamics of cortical astrocytic networks in vivo. *PLoS Biol* 2:E96.
- Iglesias R, Dahl G, Qiu F, Spray DC, Scemes E. 2009. Pannexin 1: The molecular substrate of astrocyte "hemichannels". *J Neurosci* 29:7092–7097.
- Kafitz KW, Meier SD, Stephan J, Rose CR. 2008. Developmental profile and properties of sulforhodamine 101–labeled glial cells in acute brain slices of rat hippocampus. *J Neurosci Methods* 169:84–92.
- Karpuk N, Burkovetskaya M, Fritz T, Angle, Kielian T. 2011. Neuroinflammation leads to region-dependent alterations in astrocyte gap junction communication and hemichannel activity. *J Neurosci*. 31:414–425.
- Kawasaki Y, Zhang L, Cheng JK, Ji RR. 2008. Cytokine mechanisms of central sensitization: Distinct and overlapping role of interleukin-1beta, interleukin-6, and tumor necrosis factor-alpha in regulating synaptic and neuronal activity in the superficial spinal cord. *J Neurosci* 28:5189–5194.
- Koulakoff A, Ezan P, Giaume C. 2008. Neurons control the expression of connexin 30 and connexin 43 in mouse cortical astrocytes. *Glia* 56:1299–1311.
- Kunzelmann P, Schröder W, Traub O, Steinhäuser C, Dermietzel R, Willecke K. 1999. Late onset and increasing expression of the gap junction protein connexin30 in adult murine brain and long-term cultured astrocytes. *Glia* 25:111–119.
- Lovatt D, Xu Q, Liu W, Takano T, Smith NA, Schnermann J, Tieu K, Nedergaard M. 2012. Neuronal adenosine release, and not astrocytic ATP release, mediates feedback inhibition of excitatory activity. *Proc Natl Acad Sci USA* 109:6265–6270.
- Lujan R, Nusser Z, Roberts JD, Shigemoto R, Somogyi P. 1996. Perisynaptic location of metabotropic glutamate receptors mGluR1 and mGluR5 on dendrites and dendritic spines in the rat hippocampus. *Eur J Neurosci* 8:1488–1500.
- Même W, Calvo CF, Froger N, Ezan P, Amigou E, Koulakoff A, Giaume C. 2006. Proinflammatory cytokines released from microglia inhibit gap junctions in astrocytes: Potentiation by beta-amyloid. *FASEB J* 20:494–496.
- Minami M, Katayama T, Satoh M. 2006. Brain cytokines and chemokines: Roles in ischemic injury and pain. *J Pharmacol Sci* 100:461–470.
- Mizuno T, Sawada M, Suzumura A, Marunouchi T. 1994. Expression of cytokines during glial differentiation. *Brain Res* 656:141–146.
- Murray CA, McGahon B, Mc Bennett S, Lynch MA. 1997. Interleukin-1 beta inhibits glutamate release in hippocampus of young, but not aged, rats. *Neurobiol Aging* 18:343–348.
- Nagy JI, Patel D, Ochalski PA, Stelmack GL. 1999. Connexin30 in rodent, cat and human brain: Selective expression in gray matter astrocytes, colocalization with connexin43 at gap junctions and late developmental appearance. *Neuroscience* 88:447–468.
- Nagy JI, Rash JE. 2000. Connexins and gap junctions of astrocytes and oligodendrocytes in the CNS. *Brain Res Brain Res Rev* 32:29–44.
- Nolte C, Matyash M, Pivneva T, Schipke CG, Ohlemeyer C, Hanisch UK, Kirchhoff F, Kettenmann H. 2001. GFAP promoter-controlled EGFP-expressing transgenic mice: a tool to visualize astrocytes and astrogliosis in living brain tissue. *Glia* 33:72–86.
- Orellana JA, Sáez PJ, Shoji KF, Schalper KA, Palacios-Prado N, Velarde V, Giaume C, Bennett MV, Sáez JC. 2009. Modulation of brain hemichannels and gap junction channels by proinflammatory agents and their possible role in neurodegeneration. *Antioxid Redox Signal* 11:369–399.
- Orellana JA, Shoji KF, Abudara V, Ezan P, Amigou E, Sáez PJ, Jiang JX, Naus CC, Sáez JC, Giaume C. 2011. Amyloid  $\beta$ -induced death in neurons involves glial and neuronal hemichannels. *J Neurosci* 31:4962–4977.
- Overstreet LS, Pasternak JF, Colley PA, Slater NT, Trommer BL. 1997. Metabotropic glutamate receptor mediated long-term depression in developing hippocampus. *Neuropharmacology* 36:831–844.
- Pannasch U, Vargová L, Reingruber J, Ezan P, Holcman D, Giaume C, Syková E, Rouach N. 2011. Astroglial networks scale synaptic activity and plasticity. *Proc Natl Acad Sci USA* 108:8467–8472.
- Park CK, Lü N, Xu ZZ, Liu T, Serhan CN, Ji RR. 2011. Resolving TRPV1- and TNF- $\alpha$ -mediated spinal cord synaptic plasticity and inflammatory pain with neuroprotectin D1. *J Neurosci* 31:15072–15085.
- Parpura V, Heneka MT, Montana V, Oliet SH, Schousboe A, Haydon PG, Stout RF Jr, Spray DC, Reichenbach A, Pannicke T, Pekny M, Pekna M, Zorec R, Verkhratsky A. 2012. Glial cells in (patho)physiology. *J Neurochem* 121:4–27.
- Pascual O, Ben Achour S, Rostaing P, Triller A, Bessis A. 2012. Microglia activation triggers astrocyte-mediated modulation of excitatory neurotransmission. *Proc Natl Acad Sci USA* 109:197–205.
- Pascual O, Casper KB, Kubera C, Zhang J, Revilla-Sanchez R, Sul JY, Takano H, Moss SJ, McCarthy K, Haydon PG. 2005. Astrocytic purinergic signaling coordinates synaptic networks. *Science* 310:113–116.
- Pelegrin P, Surprenant A. 2006. Pannexin-1 mediates large pore formation and interleukin-1beta release by the ATP-gated P2X7 receptor. *EMBO J* 25:5071–5082.
- Perea G, Araque A. 2010. Glia modulates synaptic transmission. *Brain Res Rev* 63:93–102.
- Poolos NP, Mauk MD, Kocsis JD. 1987. Activity-evoked increases in extracellular potassium modulate presynaptic excitability in the CA1 region of the hippocampus. *J Neurophysiol* 58:404–416.
- Ransom BR, Giaume C. 2013. Gap junctions, hemichannels. In: Kettenmann H, Ransom BR, editors. *Neuroglia*, 3rd ed. Oxford: Oxford University Press. pp 292–305.
- Retamal MA, Froger N, Palacios-Prado N, Ezan P, Sáez PJ, Sáez JC, Giaume C. 2007. Cx43 hemichannels and gap junction channels in astrocytes are regulated oppositely by proinflammatory cytokines released from activated microglia. *J Neurosci* 27:13781–13792.
- Rossi D, Volterra A. 2009. Astrocytic dysfunction: insights on the role in neurodegeneration. *Brain Res Bull* 80:224–232.
- Rouach N, Koulakoff A, Abudara V, Willecke K, Giaume C. 2008. Astroglial metabolic networks sustain hippocampal synaptic transmission. *Science* 322:1551–1555.
- Roux L, Benchenane K, Rothstein JD, Bonvento G, Giaume C. 2011. Plasticity of astroglial networks in olfactory glomeruli. *Proc Natl Acad Sci USA* 108:18442–18446.

- Santello M, Bezzi P, Volterra A. 2011. TNF $\alpha$  controls glutamatergic gliotransmission in the hippocampal dentate gyrus. *Neuron* 69:988–1001.
- Santello M, Volterra A. 2012. TNF $\alpha$  in synaptic function: switching gears. *Trends Neurosci* 35:638–647.
- Sawada M, Kondo N, Suzumura A, Marunouchi T. 1989. Production of tumor necrosis factor-alpha by microglia and astrocytes in culture. *Brain Res* 491:394–397.
- Scemes E, Spray DC, Meda P. 2009. Connexins, pannexins, innexins: Novel roles of "hemi-channels". *Pflugers Arch* 457:1207–1226.
- Schalper KA, Sánchez HA, Lee SC, Altenberg GA, Nathanson MH, Sáez JC. 2010. Connexin 43 hemichannels mediate the Ca<sup>2+</sup> influx induced by extracellular alkalization. *Am J Physiol Cell Physiol* 299:C1504–C1515.
- Schnell C, Hagos Y, Hülsman S. 2012. Active sulforhodamine 101 uptake into hippocampal astrocytes. *PLoS One* 7:e49398.
- Sofroniew MV. 2005. Reactive astrocytes in neural repair and protection. *Neuroscientist* 11:400–407.
- Suadcani SO, Iglesias R, Wang J, Dahl G, Spray DC, Scemes E. 2012. ATP signaling is deficient in cultured Pannexin1-null mouse astrocytes. *Glia* 60:1106–1116.
- Teubner B, Michel V, Pesch J, Lautermann J, Cohen-Salmon M, Söhl G, Jahnke K, Winterhager E, Herberhold C, Hardelin JP, Petit C, Willecke K. 2003. Connexin30 (Gjb6)-deficiency causes severe hearing impairment and lack of endocochlear potential. *Hum Mol Genet* 12:13–21.
- Theis M, Söhl G, Speidel D, Kühn R, Willecke K. 2003. Connexin43 is not expressed in principal cells of mouse cortex and hippocampus. *Eur J Neurosci* 18:267–274.
- Thompson RJ, Jackson MF, Olah ME, Rungta RL, Hines DJ, Beazely MA, MacDonald JF, MacVicar BA. 2008. Activation of pannexin-1 hemichannels augments aberrant bursting in the hippocampus. *Science* 322:1555–1559.
- Thompson RJ, MacVicar BA. 2008. Connexin and pannexin hemichannels of neurons and astrocytes. *Channels (Austin)* 2:81–86.
- Verkhatsky A, Sofroniew MV, Messing A, deLanerolle NC, Rempe D, Rodríguez JJ, Nedergaard M. 2012. Neurological diseases as primary gliopathies: A reassessment of neurocentrism. *ASN Neurol* 4:pii: e00082.
- Volterra A, Steinhäuser C. 2004. Glial modulation of synaptic transmission in the hippocampus. *Glia* 47:249–257.
- Wallraff A, Köhling R, Heinemann U, Theis M, Willecke K, Steinhäuser C. 2006. The impact of astrocytic gap junctional coupling on potassium buffering in the hippocampus. *J Neurosci* 26:5438–5447.
- Wang J, Ma M, Locovei S, Keane RW, Dahl G. 2007. Modulation of membrane channel currents by gap junction protein mimetic peptides: size matters. *Am J Physiol Cell Physiol* 293:C1112–C1119.
- Wang N, De Bock M, Antoons G, Gadicherla AK, Bol M, Decrock E, Evans WH, Sipido KR, Bukauskas FF, Leybaert L. 2012. Connexin mimetic peptides inhibit Cx43 hemichannel opening triggered by voltage and intracellular Ca<sup>2+</sup> elevation. *Basic Res Cardiol* 107:304.
- Wood PL. 1994. Differential regulation of IL-1 alpha and TNF-alpha release from immortalized murine microglia (BV-2). *Life Sci* 55:661–668.
- Yang S, Liu ZW, Wen L, Qiao HF, Zhou WX, Zhang YX. 2005. Interleukin-1beta enhances NMDA receptor-mediated current but inhibits excitatory synaptic transmission. *Brain Res* 1034:172–179.
- Ye ZC, Wyeth MS, Baltan-Tekkok S, Ransom BR. 2003. Functional hemichannels in astrocytes: A novel mechanism of glutamate release. *J Neurosci* 23:3588–3596.
- Yrjänheikki J, Keinänen R, Pellikka M, Hökfelt T, Koistinaho J. 1998. Tetracyclines inhibit microglial activation and are neuroprotective in global brain ischemia. *Proc Natl Acad Sci USA* 95:15769–15774.
- Zhang H, Dougherty PM. 2011. Acute inhibition of signalling phenotype of spinal GABAergic neurons by tumour necrosis factor-alpha. *J Physiol* 589:4511–4526.